journal

J. Am. Ceram. Soc., 92 [9] 1901–1920 (2009)
DOI: 10.1111/j.1551-2916.2009.03278.x

The Tetragonal-Monoclinic Transformation in Zirconia: Lessons Learned and Future Trends

Jérôme Chevalier and Laurent Gremillard†

University of Lyon, INSA-Lyon, MATEIS, Villeurbanne FR-69621, France

Anil V. Virkar

Department of Material Science & Engineering, University of Utah, Salt Lake City, Utah 84112

David R. Clarke

School of Engineering and Applied Sciences, Harvard University, Cambridge, Massachusetts 02138

Zirconia ceramics have found broad applications in a variety of energy and biomedical applications because of their unusual combination of strength, fracture toughness, ionic conductivity, and low thermal conductivity. These attractive characteristics are largely associated with the stabilization of the tetragonal and cubic phases through alloying with aliovalent ions. The large concentration of vacancies introduced to charge compensate of the aliovalent alloying is responsible for both the exceptionally high ionic conductivity and the unusually low, and temperature independent, thermal conductivity. The high fracture toughness exhibited by many of zirconia ceramics is attributed to the constraint of the tetragonal-to-monoclinic phase transformation and its release during crack propagation. In other zirconia ceramics containing the tetragonal phase, the high fracture toughness is associated with ferroelastic domain switching. However, many of these attractive features of zirconia, especially fracture toughness and strength, are compromised after prolonged exposure to water vapor at intermediate temperatures (~30°–300°C) in a process referred to as low-temperature degradation (LTD), and initially identified over two decades ago. This is particularly so for zirconia in biomedical applications, such as hip implants and dental restorations. Less well substantiated is the possibility that the same process can also occur in zirconia used in other applications, for instance, zirconia thermal barrier coatings after long exposure at high temperature. Based on experience with the failure of zirconia femoral heads, as well as studies of LTD, it is shown that many of the problems of LTD can be mitigated by the appropriate choice of alloying and/or process control.

D. J. Green—contributing editor

Manuscript No. 26208. Received April 27, 2009; approved 1 July 2009.
†Author to whom correspondence should be addressed. e-mail: laurent.gremillard@insa-lyon.fr

I. Introduction

Zirconia has been one of the most important ceramic materials for well over a century but the discovery of transformation toughening in 1975[1] heralded new visions for new high-performance applications of zirconia, ranging from bearing and wear applications to thermal barrier coatings (TBCs) to, most recently, biomedical applications. The subsequent discovery that zirconia could also be toughened by ferroelastic switching[2] gave further confidence in the application of zirconia ceramics in critical applications. Nevertheless, despite the success of zirconia in many new applications, it has become apparent that certain zirconia compositions can also have an Achilles heel, namely their propensity to low-temperature degradation (LTD) in the presence of moisture. This is a kinetic phenomenon in which polycrystalline tetragonal material slowly transforms to monoclinic zirconia over a rather narrow but important temperature range, typically room temperature to around 400°C, depending on the stabilizer, its concentration, and the grain size of the ceramic. The transformation occurs by a nucleation and growth process and typically begins at the surfaces of polycrystalline ceramics. It has all the characteristics of being an isothermal martensite. Also, although there continues to remain some uncertainty as to the precise mechanism by which moisture causes destabilization of the tetragonal phase, the observation that the kinetics of LTD are similar to those of oxygen vacancy diffusion suggests that the transformation occurs by the indiffusion of a moisture species with an activation energy similar to that of oxygen vacancy diffusion. In practical terms, LTD is, in effect, an alternative to crack propagation, stress-induced transformation for the transformation from metastable tetragonal to monoclinic (*t–m*) zirconia (see Fig. 1).

In this feature article we describe the role of phase transformations responsible for the impressive combination of mechanical properties of zirconia, their relationship to equilibrium and metastable phase diagrams, and the phenomenon of LTD. We include the effects of transformations at free surfaces because these affect the surface finish that is important for many

Feature

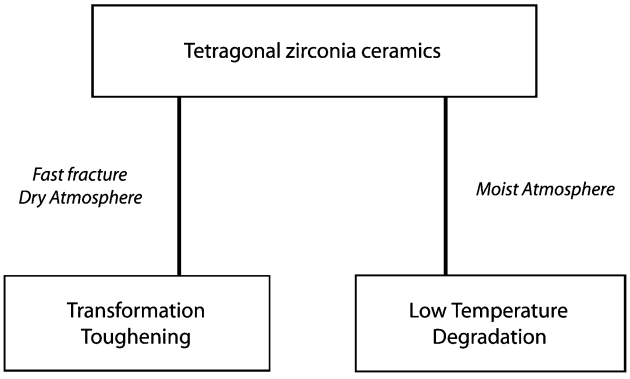

Fig. 1. Crack propagation-induced transformation and intermediate temperature exposure to moisture are two alternative means by which metastable tetragonal phase can transform to monoclinic phase.

applications as well as the kinetics. We also describe approaches being taken to avoid LTD, or minimize it, based on lessons learnt from investigation of LTD in femoral implants and the mechanisms that control it. Much of this article is concerned with the properties of the zirconia–yttria material system because the majority of the research and development that has been performed on zirconia in the last three decades has been on yttria-stabilized zirconia (YSZ). YSZ ceramics have the best combination of toughness and strength of any of the stabilized zirconias. Also, and this cannot be overemphasized, it is undoubtedly due to the early and continued availability of high-purity, uniform submicrometer particle size powders from companies such as Tosoh in Japan.

II. Experimental Procedure

The principal properties of zirconia are well known and various aspects have been reviewed in detail many times since the discovery of transformation toughening by Garvie *et al.*[1] in calcia-stabilized zirconia. For this reason, in this section we summarize only the principal features of the stabilization of zirconia, the crystallography of stabilized zirconia, and the relationship between mechanical properties and the phase transformations in zirconia. The panels describe the essentials of phase equilibria and the transformation crystallography.

Pure zirconium oxide exhibits three allotropes: monoclinic (*m*), which is the stable phase up to 1170°C, where it transforms to tetragonal (*t*), and then cubic (*c*) at temperatures above 2370°C. A comprehensive review of the different structures for zirconia can be found in Green *et al.*[3] The *t*−*m* transformation, which is martensitic, has been the subject of the most careful attention, because it usually occurs during the sintering and on both heating and cooling. The *t*−*m* transformation is accompanied by a large shear strain and a large volume increase (see Panel B). Together these create large internal stresses on cooling. So large, in fact, that pure zirconia sintered above 1170°C inevitably disintegrates by cracking upon cooling. To maintain the integrity of sintered zirconia bodies at room temperature, one can either sinter at low temperature for it to remain monoclinic during sintering—which leads to a low-strength and toughness ceramic—or stabilize the tetragonal or the cubic phases at room temperature by alloying, thereby avoiding the *t*−*m* transformation during cooling. The fundamental approach to the engineering use of zirconia and avoiding the transformation-induced cracking described by Ruff and Ebert[4] almost a century ago remains valid today: alloying pure zirconia with another oxide to fully or partially stabilize the tetragonal and/or the cubic phase. Calcium, magnesium, yttrium, and cerium oxides have been the most widely used stabilizers and lead to a number of different microstructures. In general, zirconia ceramics may conveniently be classified into three major types according to their microstructure: FSZ, PSZ, and TZP, standing, respectively, for fully stabilized zirconia, partially stabilized zirconia, and tetragonal zirconia polycrystals. In FSZ zirconia is in its cubic form, the form most commonly used in oxygen sensors and fuel cell electrolytes. It is generally obtained with large concentration of stabilizers (i.e., more than 8 mol% Y_2O_3). The PSZ consists of nanosized tetragonal or monoclinic particles that have precipitated out in a cubic matrix. Such zirconia ceramics are generally obtained with the addition of lime or magnesia. TZPs are often considered as monoliths of tetragonal phase, although they may contain a secondary cubic phase (see Panel A). The majority of TZPs that have been investigated are those stabilized with yttria or ceria.

III. Stabilization and Transformation of the Tetragonal Phase

As mentioned above, stabilization of powders and sintered ceramics can be achieved by alloying pure zirconia with other oxides. Investigations of the stability of different phases with different stabilizers led to the development of the equilibrium phase diagrams such as those compiled by the American Ceramic Society—NIST project.[15]

Alloy stabilization not only enables fabrication of crack-free zirconia but as demonstrated by Gupta *et al.*,[16] sintered bodies of polycrystalline tetragonal zirconia can be prepared and the tetragonal phase retained down to room temperature even though the equilibrium phase is monoclinic. These metastable tetragonal ceramics exhibited exceptional fracture toughness when the transformation to the monoclinic phase was triggered by a propagating crack. The toughening that can be achieved for different concentrations of yttria is illustrated in Fig. 2, which summarizes data for transformation-toughened zirconia and ferroelastic toughening. Also shown, superimposed, is the sensitivity to aging as a function of yttria concentration. The fracture toughness of monoclinic and cubic zirconia, which is similar to that of window glass, provides a reference against which the toughening through the *t*−*m* phase transformation can be compared. It is emphasized that the data are obtained from standard fracture toughness tests, such as indentation and double cantilever beam tests, in fast fracture conditions under which LTD is avoided. As indicated in Fig. 2, the attainable fracture toughness decreases as the yttria concentration increases. In the context of the metastable phase diagram, the toughening is proportional to the magnitude of the undercooling below the T_0 (t/m) temperature (see Panel A for a more detailed explanation). Furthermore, transformation toughening is restricted to moderate temperatures, becoming ineffective when the stable phase is tetragonal and not monoclinic. For these reasons, the most attractive compositions for transformation toughening are those with low yttria concentrations (but high enough to prevent spontaneous *t*−*m* transformation during cooling), typically 2–3 mol% Y_2O_3.

In the presence of moisture, the transformation of metastable *t*–*m* can alternatively occur without the passage of a crack. In this sense, LTD is a competing process to transformation toughening with the two providing limiting behaviors by which the metastable tetragonal phase transforms to the more stable monoclinic phase (Fig. 1). If the transformation is triggered by a propagating crack, then one can get enhanced toughening (see "Section III*(2)*"). On the other hand, the transformation may be triggered "chemically" by the infusion of water-derived species from the surface. The process on a surface is complex (Fig. 3) and results not only in the undesirable transformation but also surface roughening, microcracking, and grain pull-out as well as loss of strength—all processes detrimental to structural applications. The dilemma facing the alloy designer is that the YSZ compositions that are the most attractive for their fracture toughness are also those that are most susceptible to LTD. This is illustrated by the comparison of the fracture toughness data with the LTD data in Fig. 2.

The stabilization of the tetragonal phase in polycrystalline ceramics is, undoubtedly, largely dependent on the mutual elastic constraint provided by the surrounding, untransformed

Panel A. Zirconia-Yttria Phase Diagram[5,6]

The zirconia–yttria phase diagram has been significantly refined many times since it was first introduced in 1951 by Duwez *et al.*[7] (The phase diagram book devoted to zirconia includes 30 different variations in the phase diagram.) At first, the succession of revisions might be a surprise but the essential difficulty is that cation diffusion in zirconia is so slow[8] that it has proved particularly difficult to establish equilibrium and hence the phase boundaries at temperatures below about 1400°C. Furthermore, the slow diffusion kinetics means that metastable extensions of the phases can readily occur. Interestingly, it was the prospect of diffusion-limited processes in zirconia that led Pol Duwez to investigate the system in his pioneering studies of rapid solidification and glass formation. In addition, the characteristic features of the martensitic transformation, such as the start and finish temperatures, have further complicated the interpretation of the diagram and the interpretation of microstructures. This uncertainty is shown in Scott's phase diagram by the hatched region.[9] As a result, there has been considerable confusion in the literature about the details of the phase diagram. Yashima *et al.*[5] present a graphic illustration of the confusion by superimposing many of the published diagrams on one another in their Fig. A1. The disagreements are particularly pronounced for the region pertinent to transformation toughening and the low-temperature degradation.

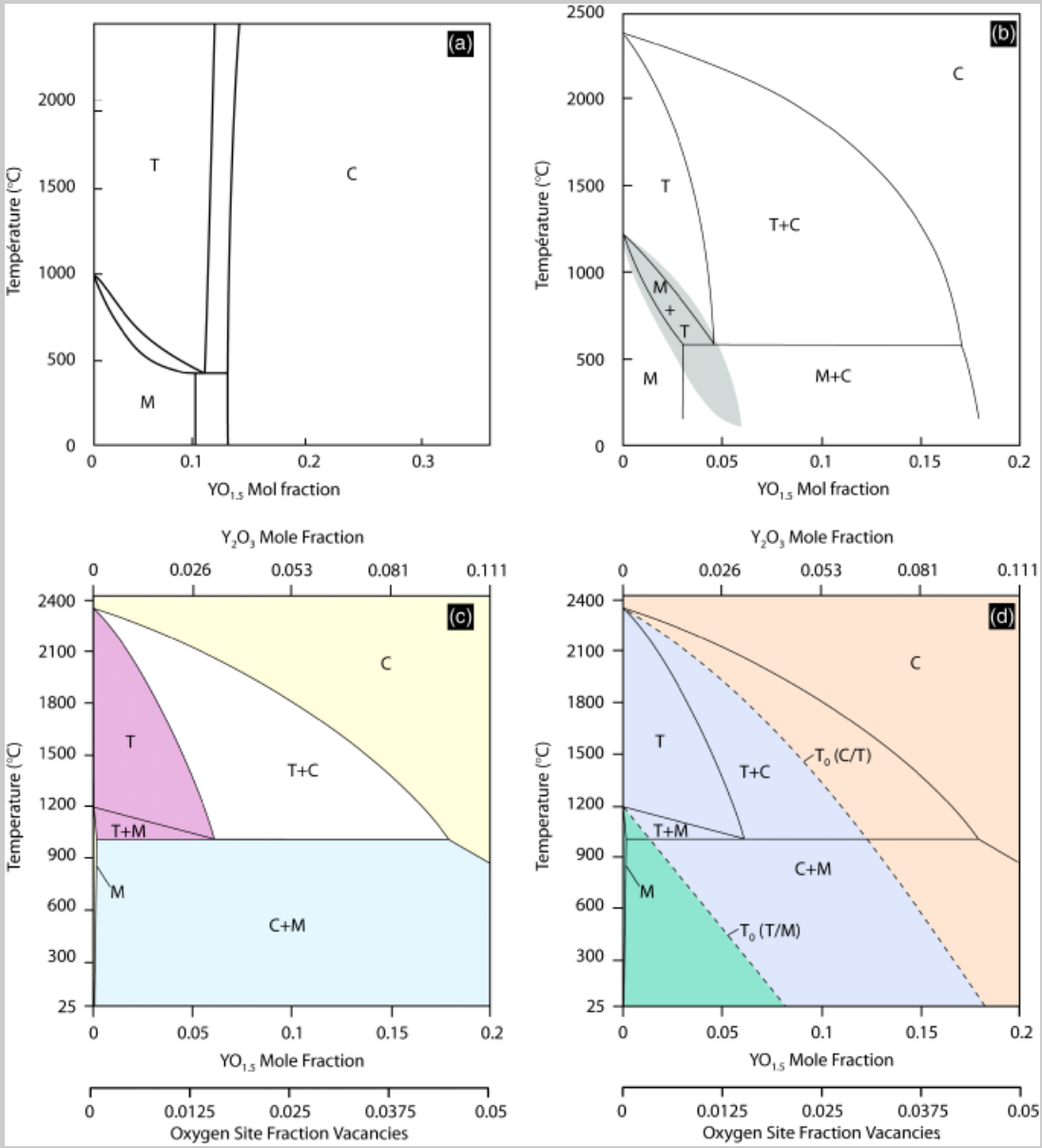

Fig. A1. Evolution in our knowledge of the zirconia–yttria phase diagram: (a) original diagram by Duwez in 1951,[6] (b) diagram presented by Scott in 1975,[8] (c) and (d) most recent diagrams[9,10] (d) is the metastable phase diagram.

The evolution in our knowledge of the phase diagram can be illustrated by the diagrams in Fig. A1, showing the original diagram by Duwez, the diagram presented by Scott in 1975[8] and the most recent diagrams that combines experimental and computational studies.[10,11] At the time of writing, there are indications that even this version may not be quite correct and that the tetragonal boundary may exhibit retrograde curvature, as occurs in the ZrO_2–CeO_2 system.[12] Considerable clarification has been obtained from computer determination of the phase diagram, particularly the position of the metastable T_0 lines. However, it has to be emphasized that the metastable lines themselves, as well as the phase boundary lines are obtained from optimization

Panel A. Continued

procedures that use the experimentally determined equilibrium phase boundaries as input parameters. For instance, the temperature of the monoclinic to tetragonal and the tetragonal to cubic, as well as the t/c boundary line are used to determine the metastable T_0 (t/m) boundary so if the t/c boundary line is inaccurate, then the computed T_0 (t/m) may not be fully correct. The necessity of considering the metastable phase diagram is that cation diffusion in zirconia is exceptionally slow at all but the highest temperature. This is illustrated by the graph in Fig. A2, which shows the estimated time for diffusion to occur to homogenize the Y content of a 0.5- or 3-μm-diameter grain at different temperatures (calculated from Kilo *et al.*[8] and[13]). Even at a temperature of 1500°C, a sintering temperature commonly used for zirconia ceramics in the past, it is estimated to take several weeks to achieve compositional homogeneity for the 3-μm-grain size material. For a 0.5-μm-grain size, this would represent days/hours instead of weeks (time roughly divided by 36 compared with the 3 μm case). This explains why phase and yttria partitioning was observed in 3Y-TZP sintered for 5 h at 1550°C in previous work.[14]

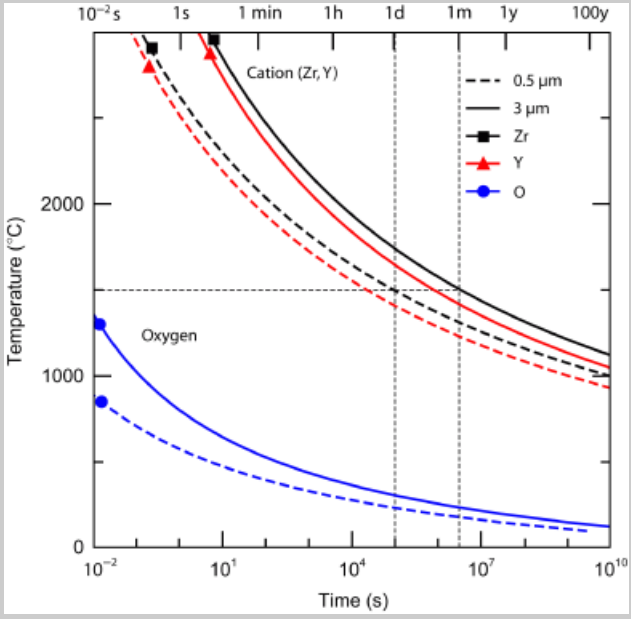

Fig. A2. Estimated time for diffusion to occur to homogenize the Y content of 0.5- and 3-μm-diameter grains at different temperatures in 3Y-TZP.[7,11] TZP, tetragonal zirconia polycrystals; Y, yttria.

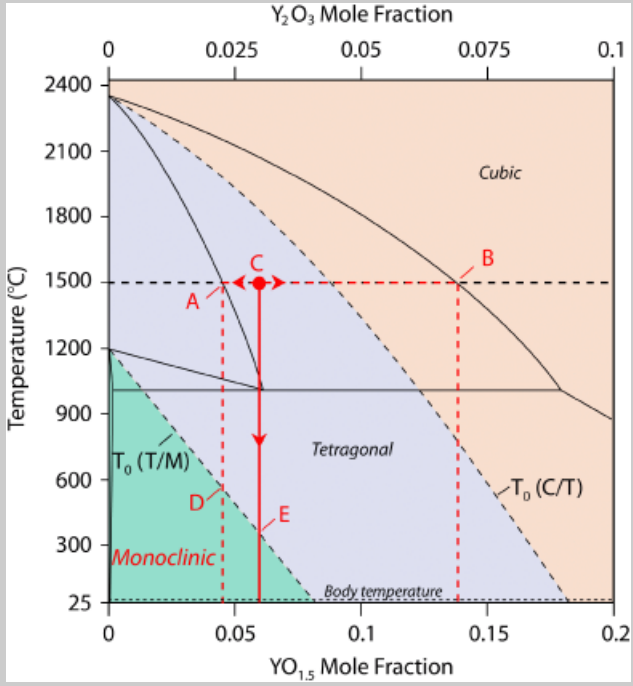

Fig. A3. Metastable zirconia–yttria phase diagram.

To illustrate the consequences of the very slow cation diffusion, and the crucial importance of the metastable phase diagram in understanding LTD, we take as an example, a 3 m/o Y_2O_3 (6.0 m/o $YO_{1.5}$) material sintered at 1500°C, composition C in Fig. A3. At equilibrium at this temperature, the sintered sample should consist of two phases, a tetragonal phase of composition 2.4 m/o Y_2O_3 (4.5 $YO_{1.5}$) (point A) and a cubic phase of composition of 7.5 m/o Y_2O_3 (point B). At room temperature, the equilibrium phases, from Fig. A1, would be a monoclinic phase with a yttria concentration of almost zero and a cubic phase with a yttria concentration of ~18 m/o Y_2O_3. However, for this equilibrium condition to occur the yttrium ions must diffuse to partition into the yttria-poor monoclinic and yttria-rich cubic phases as shown by the horizontal arrows in the figure. As the indicated by the diffusion distance figure, this would take many years. Instead, under typical cooling conditions, little or no yttrium ion partitioning occurs and the compositions obtained on cooling to room temperature, will be given by the intersection of the vertical dashed lines with the composition axis. At temperatures below the T_0 (t/m), the tetragonal phase is metastable with respect to transformation to the monoclinic but the transformation is kinetically limited. For instance, if there has been no diffusion, the T_0 (t/m) temperature is given by the intersection point E whereas if diffusional partitioning is complete at the sintering temperature, then the T_0 (t/m) temperature is given by the intersection point D. Consequently, before low-temperature aging, the phases observed will then be a metastable tetragonal phase and a cubic phase, both with the same yttria concentrations as they have at the sintering temperature. Then, as the transformation occurs below the T_0 (t/m) temperature, the monoclinic phase will have the same yttria concentration as the tetragonal phase, namely 2.4 m/o Y_2O_3 (4.5 $YO_{1.5}$) in this example. Interestingly, as the yttria stabilizer concentration is increased and no partitioning occurs, the T_0 (t/m) temperature decreases until at about 3.6 m/o Y_2O_3 (7.0 m/o $YO_{1.5}$), it falls to below room temperature. So, unless the material is first transformed to the equilibrium cubic and tetragonal phases during sintering and subsequent heat treatment, it will not be susceptible to transformation until lower temperature is attained.

A further consequence of the equilibrium t/m phase boundary is that its steep slope implies that the composition of the tetragonal phase formed by diffusional partitioning at high temperatures is not very sensitive to the average composition of the powders, and hence there is little variation in the T_0 (t/m) temperature with the yttria content. What does change are the relative volume fractions of the tetragonal and cubic phases at the sintering temperature, and hence the maximum volume fraction of tetragonal that can transform to monoclinic by either transformation toughening or moisture-mediated LTD.

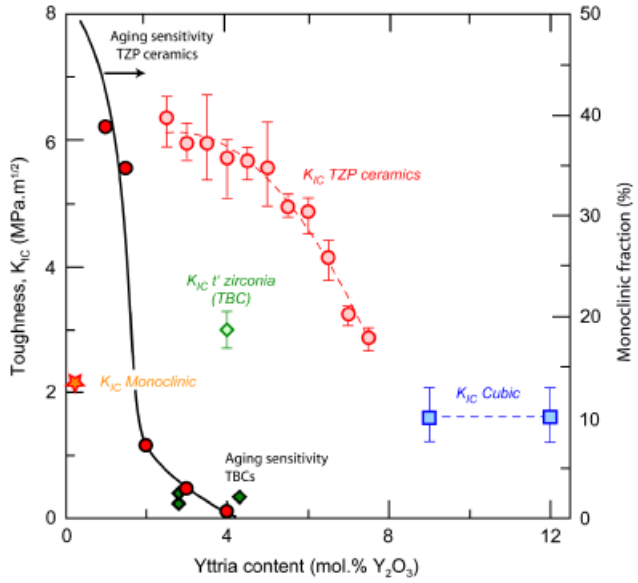

Fig. 2. Fracture toughness and aging sensitivity of yttria-stabilized zirconia as a function of yttria stabilizer concentration. Toughness data for cubic and monoclinic zirconia is indicated together with the ferroelastic toughness in a densified thermal barrier coating. Aging sensitivity is here described by the degree of tetragonal phase transformation toward monoclinic (i.e., the ratio monoclinic fraction/initial tetragonal fraction) after 3 h at 134°C in water vapor.

grains, whether these are also tetragonal grains, as in TZP, or the cubic matrix material in which the tetragonal precipitates are embedded for the PSZ ceramics. As the $t-m$ transformation is accompanied by a volume increase, the transformation is constrained by the surrounding grains. In these cases, the thermodynamic framework that includes mechanical work arguments provides a rationale for the stabilization. The most general description of the energetics involved is reproduced below.

Recently with detailed study of zirconia nanoparticles, Garvie's claim[17] that pure, zirconia powders could be retained in the tetragonal state provided that their size was below a critical size has been extensively validated. Garvie's concept was that stabilization could occur by surface energy alone and a series of energy cross-overs between monoclinic, tetragonal, and cubic phases has since been demonstrated as being consistent with the dominant role of surface energy at nanometer particle sizes. For example, a 4–24 nm stability range of tetragonal zirconia at room temperature can be extrapolated from Pitcher *et al.*'s work,[18] while monoclinic phase is stable above this size. This role of surface energy is confirmed by Suresh *et al.*,[19] who found a decrease of the $t-m$ transformation temperature upon cooling with grain size.

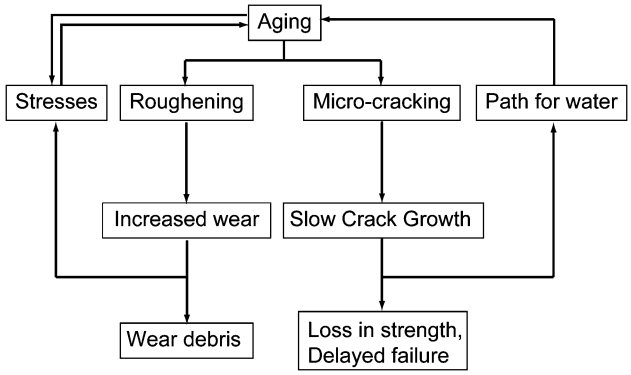

Fig. 3. Potential effect of aging on the integrity of zirconia devices. Arrows indicate coupling of aging with crack propagation and wear mechanisms.

While the stabilization of pure zirconia can be understood in terms of the balance between chemical and surface energy, the reason that different aliovalent ions are effective as stabilizers and also, perhaps, why moisture causes destabilization and isothermal transformation from tetragonal to monoclinic remains to be understood. Many researchers have argued that stabilization is a direct consequence of the presence of the oxygen vacancies introduced by the aliovalent alloying element rather than the aliovalent dopant itself.[20,21] However, this hypothesis could not be tested until the advent of large-scale computations. Now, it has been shown computationally[22] that the tetragonal phase can be produced with lower energy than the monoclinic phase by introducing oxygen vacancies and without any aliovalent ions into the unit cell. This form of stabilization alone is unlikely to be the complete explanation because the solubility of the tetragonal and cubic phases at different temperatures depends on the alloying dopant. Otherwise, all the phase diagrams for different stabilizers would collapse onto one when plotted as a function of concentration of oxygen vacancies. Nevertheless, it is an attractive explanation that has been used to rationalize the prevailing explanation of LTD (see "Section IV"): that moisture species enter into the tetragonal lattice, annihilating oxygen ion vacancies and thereby destabilizing the tetragonal (and cubic phases).

The most systematic study of the role of different stabilizer (dopant) ions on the stability of tetragonal and cubic zirconia has been performed using X-ray absorption spectroscopy and results published in a series of papers by Li *et al.*[20,23] They examined the effect of trivalent and tetravalent dopant ions, and the effect of undersized and oversized dopants on the local environment of zirconium ions. Local atomic structures around the Zr^{4+} and around dopant cations in zirconia solid solutions were determined. These included undersized (Fe^{3+}, Ga^{3+}) and oversized (Y^{3+}, Gd^{3+}) trivalent ions as well as undersized (Ge^{4+}) and oversized (Ce^{4+}) tetravalent ions.

In the case of trivalent dopants, oxygen vacancies are generated for charge compensation. It was concluded that the vacancies are associated with the Zr cations in the case of oversized dopants, and with the two dopant cations in the case of undersized dopants. Both configurations favor sevenfold coordinated oxygen ions around the Zr cations and stabilize the tetragonal or even the cubic phases. However, the different availability of oxygen vacancies to Zr is responsible for the more effective stabilization effects of oversized trivalent dopants. In essence, the stabilization of tetragonal zirconia with oversized trivalent cations is twice as efficient as with undersized trivalent cations. From the results and the analysis performed by Li and colleagues, it is evident that doping by trivalent oversized cations, such as Y^{3+}, is most efficient in relieving the oxygen overcrowding (via both oxygen vacancies generation and dilatation of the cation network). The conceptual idea being that oxygen overcrowding around the small zirconium Zr^{4+} cation is responsible for the poor stability of undoped tetragonal zirconia, and that the tetragonal phase may be stabilized by oxygen vacancies adjacent to the Zr^{4+} ion and introduced by aliovalent doping. This also provides a conceptual explanation for the stabilization by dilatation of the cation structure, and explains why 1.5 mol% of Y_2O_3 is sufficient to stabilize tetragonal zirconia, whereas 10 mol% of CeO_2 is needed to achieve the same stability. Recent work[24] using ^{89}Y NMR has provided more direct experimental support for the preference of oxygen vacancies to reside in lattice sites adjacent to the Zr^{4+} ion in YSZ alloys.

(1) The Energetics of Transformation

The foregoing discussion describes the stabilization of tetragonal and cubic phases of zirconia under stress-free conditions. For polycrystalline ceramics, where the tetragonal phase is retained, transformation is mechanically constrained under metastable conditions. The condition for transformation can be expressed in terms of the different energy contributions to the overall energy, as discussed by Lange,[25] who considered the

energy of a tetragonal particle embedded in an infinite matrix. Although a rather idealized configuration that does not take into account the presence of a free surface or irregular shapes grains, this simple analysis provides considerable insight into the factors affecting the transformation of the particle to its monoclinic allotrope. The change of total free energy (ΔG_{t-m}) for the $t-m$ transformation of the particle can be expressed by

$$\Delta G_{t-m} = \Delta G_c + \Delta U_{SE} + \Delta U_S \quad (1)$$

where ΔG_c (<0 at temperatures below the equilibrium M_S temperature) is the difference in chemical free energy between the tetragonal and monoclinic phases. This is dependent on temperature and composition, implicitly including the oxygen vacancy content. The term ΔU_{SE} (>0) refers to the change in elastic strain energy associated with the transformation of particles. This is dependent on the modulus of the surrounding matrix, the size and shape of the particle, and the presence of internal or external stresses. The final term, ΔU_S (>0) is the change in energy associated with the formation of new interfaces when the transformation occurs, for instance, cracks and monoclinic variants. The particle remains in its tetragonal state if the overall thermodynamic driving force $\Delta G_{t-m}>0$, i.e. if $|\Delta G_c| < \Delta U_{SE} + \Delta U_S$. When ΔG_{t-m} becomes negative, the tetragonal particle is metastable or unstable and may transform into its monoclinic state. By decreasing $|\Delta G_c|$ and increasing ΔU_{SE}, the addition of Y_2O_3 decreases the driving force of $t-m$ transformation, hence its temperature (see yttria–zirconia phase diagram in Panel A), making possible the retention of metastable tetragonal phase in dense bodies at room temperatures. The elastic self-energy ΔU_{SE} is directly related to the surrounding matrix modulus, so having the matrix of a stiffer material, such as alumina, increases ΔU_{SE}, stabilizing the tetragonal phase. It is also directly influenced by applied or internal stresses: tensile hydrostatic stress will act to reduce ΔU_{SE}, destabilizing the tetragonal phase, whereas hydrostatic pressure favors the retention of the tetragonal phase. One of the consequences of these contributions is that the driving force for the $t-m$ transformation will not be the same inside the bulk and on its surface (or even for powders), because neither ΔU_{SE} nor ΔU_S are the same. In particular, there can be configurations at the surface where the volume change of the transformation can be accommodated by a surface uplift (Panel B). This accommodation is not possible in the bulk. (The main features of the tetragonal to monoclinic transformation at the surface and the bulk are schematized in Panel B.) There is also the possibility

Panel B. Main Features of the Tetragonal to Monoclinic Transformation in Zirconia

Crystallography of the transformation.

The tetragonal to monoclinic phase transformation in zirconia is martensitic in nature. Even if alternative approaches[29] have been recently developed, it is most often described by the phenomenological theory of martensitic crystallography (PTMC). The reader may refer to the work of Kelly and Rose[30] or of Deville *et al.*[31] for a comprehensive description.

Crystallographic correspondences exist between the parent (tetragonal) and the product (monoclinic) phase, as schematized in Fig. B1. They can be described by habit planes and directions (shape strain) as summarized in Table B1.[31] Three possible lattice correspondences exist, called ABC, BCA, and CAB, which correspond to a change of the (a_t, b_t, c_t) lattice axis of the tetragonal phase changes into (a_m, b_m, c_m), (b_m, c_m, a_m) and (c_m, a_m, b_m), respectively. Each of these lattice correspondences may occur along two different habit planes. This leads to the six different configurations given in Table B1 and schematized in Fig. B2. The configurations depicted in Fig. B2 take into account the fact that four variants may occur for each crystallographic correspondence (indeed, in the tetragonal symmetry, a, b, $-a$ and $-b$ are crystallographically equivalent). For each, the shear strain associated to the tetragonal to monoclinic (t–m) transformation is around 0.16 and the volume expansion around 0.05.

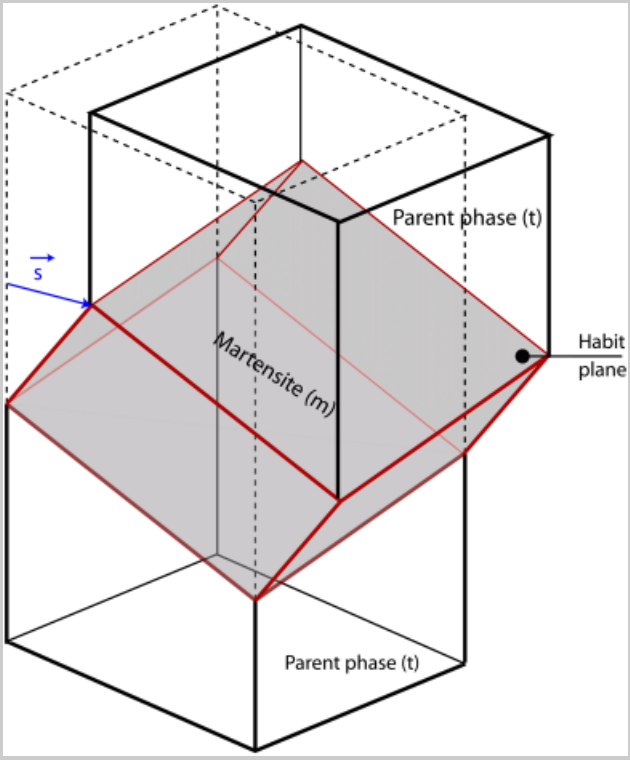

Fig. B1. Schematic illustration of crystallographic correspondences between the tetragonal (parent) and the monoclinic (product) phases during the martensitic $t-m$ transformation. $t-m$, tetragonal to monoclinic.

Table B1. Crystallographic Features of the Tetragonal–Monoclinic Martensitic Transformation in Zirconia[31]

Lattice correspondence	Lattice invariant shear†	Magnitude of g	Habit plane normal‡	Shape strain‡	Shape strain amplitude	Shear component	Volume change
ABC 1	$(011)[0\bar{1}1]$	0.0344	$\begin{bmatrix}-0.9537\\0.0055\\0.3005\end{bmatrix}$	$\begin{bmatrix}-0.0026\\0.0028\\0.1640\end{bmatrix}$	0.1640	0.1556	0.0518
ABC 2	$(011)[0\bar{1}1]$	0.0344	$\begin{bmatrix}0.0915\\-0.0171\\-0.9956\end{bmatrix}$	$\begin{bmatrix}0.1597\\-0.0007\\-0.0373\end{bmatrix}$	0.1640	0.1556	0.0518
BCA 1	$(110)[1\bar{1}0]$	0.0344	$\begin{bmatrix}0.0034\\0.3935\\-0.9193\end{bmatrix}$	$\begin{bmatrix}0.0030\\0.1751\\0.0186\end{bmatrix}$	0.1761	0.1683	0.0518
BCA 2	$(110)[1\bar{1}0]$	0.0344	$\begin{bmatrix}-0.0168\\-0.9996\\-0.0241\end{bmatrix}$	$\begin{bmatrix}-0.0004\\-0.0558\\0.1670\end{bmatrix}$	0.1761	0.1683	0.0518
CAB 1	$(101)[10\bar{1}]$	0.0027	$\begin{bmatrix}0.3006\\-0.9537\\-0.0001\end{bmatrix}$	$\begin{bmatrix}0.1640\\-0.0026\\-0.0002\end{bmatrix}$	0.1640	0.1556	0.0518
CAB 2	$(101)[10\bar{1}]$	0.0027	$\begin{bmatrix}-0.9958\\0.0915\\0.0003\end{bmatrix}$	$\begin{bmatrix}-0.0373\\0.1597\\0.0001\end{bmatrix}$	0.1640	0.1556	0.0518

Input parameters: t-phase: $a_t = 5.128$ Å, $c_t = 5.224$ Å; m-phase: $a_m = 5.203$ Å, $b_m = 5.217$ Å, $c_m = 5.388$ Å, $\beta_m = 98.91°$. †Expression in the lattice axis system of the tetragonal parent phase. ‡Expression in the orthogonal axis system bounded to the tetragonal lattice axis system.

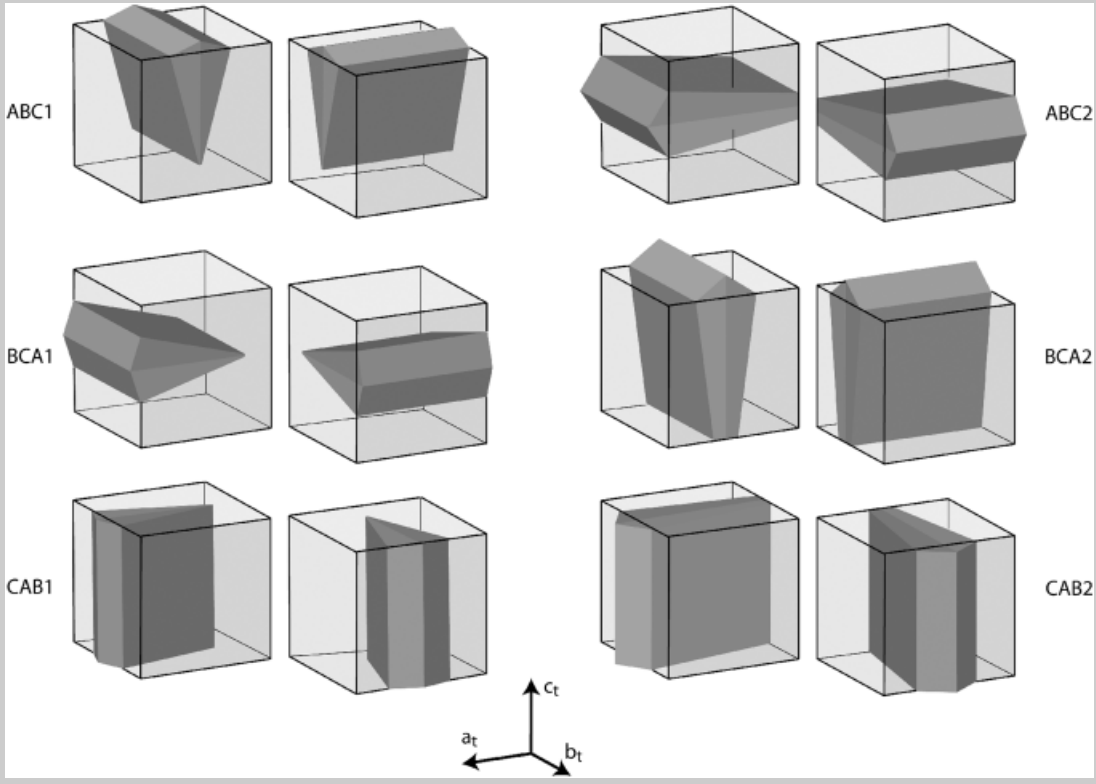

Fig. B2. Self-accommodating variant pairs deduced from the different lattice correspondences with the effect of $t-m$ transformation on a surface perpendicular to the junction plane.[31] $t-m$, tetragonal to monoclinic.

Features of the transformation at the surface

Recently, atomic force microscopy (AFM) brought new insights into the transformation induced relief. A typical example of surface uplift associated to the onset of transformation in a ceria-stabilized zirconia is given in Fig. B3. The relief exhibits fourfold symmetry, with a set of four variants. This indicates that the free surfaces where the observations are done are nearly perpendicular to the c_t-axis. Among the six possible configurations of Fig. B2, only ABC1 and BCA2 present the most important shape strain along the c_t-axis. In the case of BCA2, however, a significant strain takes place along the b_t-axis too, which would lead to important internal stresses. Therefore ABC1 is the most likely to occur in practice at the surface, because all the volume increase associated to the transformation is relaxed through a surface uplift. In other words, for such configuration

Panel B. Continued

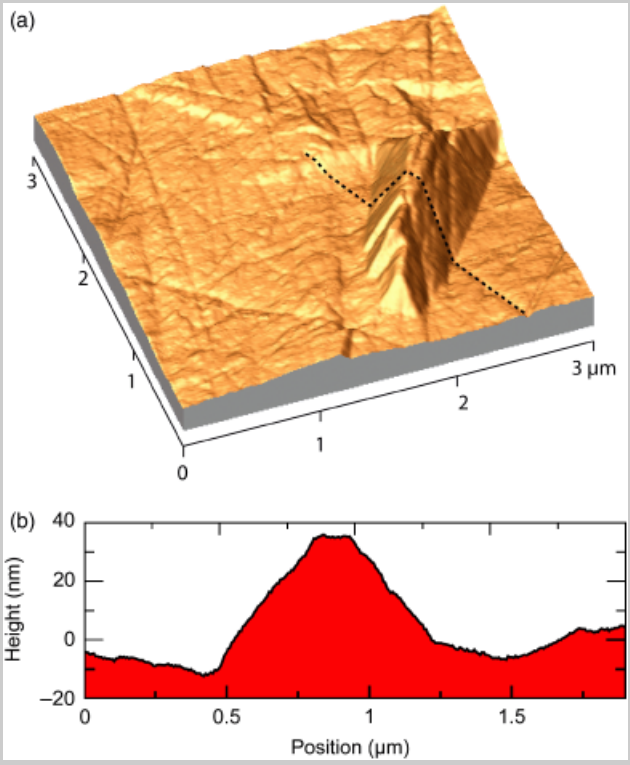

Fig. B3. surface uplifts associated to the onset of transformation in a ceria-stabilized zirconia.[30]

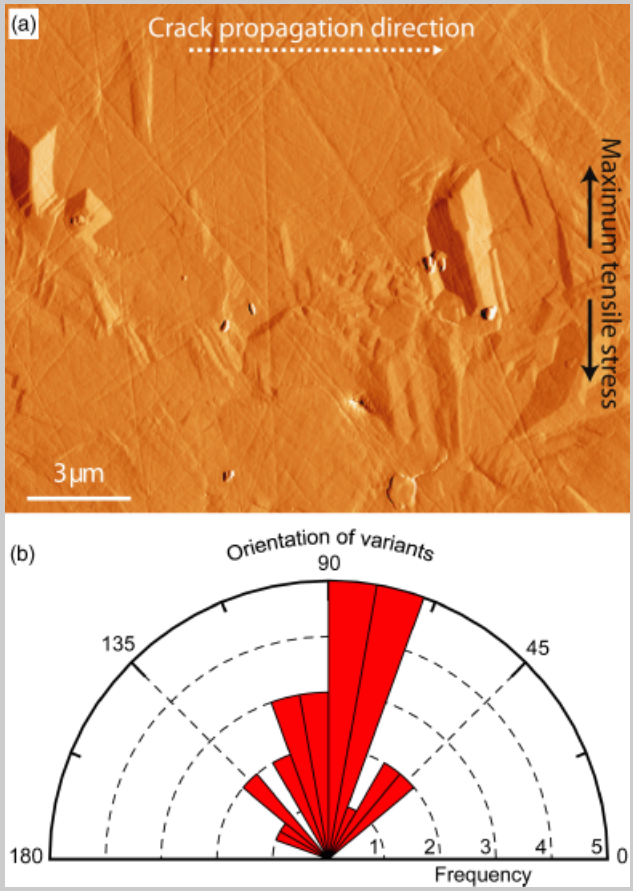

Fig. B4. Surface uplifts associated to the $t-m$ transformation in a ceria-stabilized zirconia in the vicinity of a propagating crack. $t-m$, tetragonal to monoclinic.

(c_t-axis perpendicular to the surface and ABC1 correspondence), the term ΔU_{SE} in Eq. (1) (elastic strain energy change due to the transformation) is close to zero. It is then obvious that the grains likely to transform first in zirconia are surface grains, and that these grains have their c_t-axis close to the normal to the surface. However, grains with their a_t-axis perpendicular to the surface may also transform following lattice correspondence CAB1, because shape strain for this correspondence is parallel to a_t. For this configuration, only two variants are susceptible to occur, leading to a topography change with a twofold symmetry only.

Features of the transformation at the surface, in the presence of stresses

In the presence of a stress field, the net driving force for the transformation can be modified. This change depends both on the nature and the magnitude of the stress field and on the orientation of the potential habit plane with respect to the stress field. Grains with their c_t-axis perpendicular to the surface and their junction planes parallel to the maximum tensile stress are the most likely to transform.[32] Figure B4 shows an AFM picture of a transformed zone around a propagating crack. Large stresses around the crack favor the transformation, and this occurs first for the grains subjected to the largest tensile stresses, with an adequate orientation.

Features of the transformation in the bulk

$t-m$ transformation in the bulk, in the presence of a stress field, is the main source of toughening in zirconia systems at room temperature.

Transmission electron microscopy (TEM) images are so far the only way to obtain the features of the transformation in the bulk and the majority of TEM studies have been performed in Mg-PSZ. Lenticular tetragonal precipitates transform into a stack of monoclinic variants, which accommodate the shear component of the transformation. Therefore, in first good approximation, only the dilatant component of the transformation contributes to toughening.

that the surface energy change ΔU_S is lower in the presence of moisture or water vapor pressure. Similarly, just as a critical size exists for the $t-m$ transformation exists in powders,[26] it may well be modified on the surface[27] or in the bulk.[25] The critical size often reported for bulk transformation is on the order of a micrometer, whereas it falls to around a nanometer at the surface.[28] This is of major implication for LTD, which may occur even in very fine zirconia ceramics.[28]

(2) Mechanics of Transformation Toughening

As described earlier, the energy required to propagate a crack through a dense zirconia-containing metastable zirconia is increased if the crack relieves some or all of the mechanical constraint on the metastable tetragonal and allows it to transform to the monoclinic phase. This can only occur below the T_0 (t/m) temperature, which in some papers is identified as the martensite start temperature, T_{M_S}. Two equivalent descriptions

of the toughening afforded by crack-tip-induced transformation have been formulated, one in terms of stress intensities and the other in terms of energies. A comprehensive review of the models and the experimental data on transformation toughening is beyond the scope of this review. The reader interested may refer to the book by Green *et al.*[3] for details. Phase transformation toughening originates in the presence of large tensile stresses around a crack, which can destabilize the tetragonal phase in the vicinity of the crack, forming a transformation zone. McMeeking and Evans[33] developed a model of phase transformation toughening at the beginning of the 1980s in which the stress-induced transformation leads to a shielding K_{Ish} of the applied stress intensity factor K_I. This means that the real stress intensity factor at the crack tip K_{Itip} is lower than that applied by the external forces, according to

$$K_{Itip} = K_I - K_{Ish} \tag{2}$$

Theoretical models[33] and experimental results[34] show that the higher the applied stress intensity factor, the larger the transformation zone and the larger the shielding effect, leading to the well-known equation

$$K_{Ish} = C_{sh} K_I \tag{3}$$

with

$$C_{sh} = \frac{0.214 E V_f e^T (1+\nu)}{(1-\nu)\sigma_m^c}\left(\frac{\sqrt{3}}{12\pi}\right)$$

In this equation, E is the Young modulus, V_f the volume fraction of transformable particles, e^T is the volume dilatation associated to the transformation, ν the Poisson ratio, and σ_m^c is the critical local stress leading to phase transformation.

The toughening capability of a given zirconia is directly dependent on the critical local stress leading to phase transformation, σ_m^c. This value, σ_m^c, depends in turn on the magnitude of the undercooling below the T_0 (t/m) temperature: the larger the undercooling below T_0 (t/m) the lower critical stress for stress assisted phase transformation and thus the larger the transformation toughening.

As mentioned in "Section I", transformation induced by crack propagation is one of a number of competing pathways by which the tetragonal phase can transform to the monoclinic form. At fast crack velocities, the rate at which atomic bonds at the crack tip are ruptured is much greater than the rate at which the environment can reach the tip. This is region III of the crack velocity vs stress intensity characteristic shown in Fig. 4.[34] When a crack is propagated in a nonreactive environment, its velocity is given by the extrapolation of region III to lower stress intensities, as illustrated by the data in Fig. 4 obtained in testing in vacuum and silicon oil. In those cases where the environment reacts with the crack-tip, region I, higher crack velocities than the extrapolation of the region III behavior result as shown in Fig. 4 for YSZ. Similar behavior is well established for fracture of glasses and several other ceramic materials, including alumina.

Data on the dependence of crack velocity on stress intensity for 3 *m/o* Y_2O_3 has been obtained at temperatures up to 75°C and exhibit an apparent threshold at $\sim 3.2\ MPa \cdot m^{1/2}$. Based on the data at this stress intensity, the crack velocity is commensurate with the rate at which the degradation front moves into a ceramic. Indeed, the temperature dependence data suggest that the activation energy for moisture-assisted crack growth is similar to that for moisture-induced LTD discussed in "Section IV."

(3) Ferro-Elastic Toughening

Another possible source of toughening in tetragonal zirconias is crack propagation-induced ferro-elastic domain switching, sometimes referred to as ferroelastic toughening. This is possible in tetragonal zirconias produced by cooling from the cubic phase by a composition invariant displacive reaction or by the direct deposition of tetragonal-prime zirconia, for instance by sputtering or electron-beam deposition. In the former case, when a cubic crystal or individual grain transforms to tetragonal, six different, crystallographically equivalent orientations of the *c*-axis of the tetragonal can result. Each of these variants ("domains") has the same energy but can re-orient when a stress is applied. In the case of tetragonal crystals formed directly, each grain can be a single domain. Then, individual grains or portions within each grain can be switched to a different orientation by an applied stress. This can occur as a result of an applied stress or in the presence of a propagating crack.

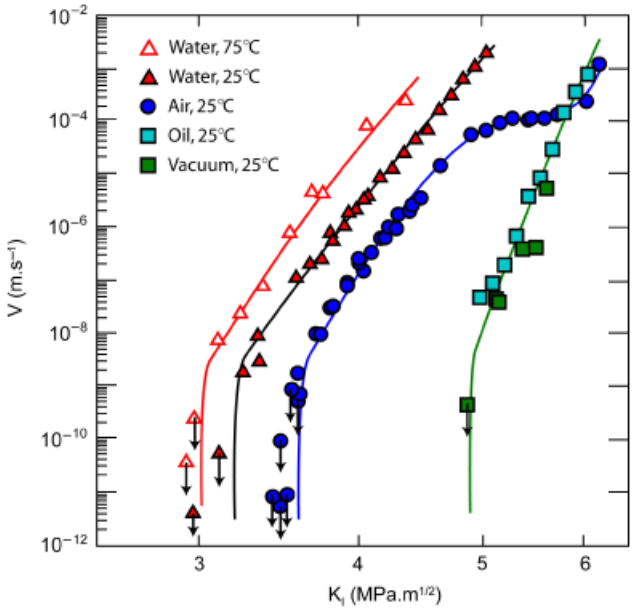

Fig. 4. V–K_I laws in 3Y-TZP. TZP, tetragonal zirconia polycrystals; Y, yttria.

For domains to reorient, an applied stress of the correct sign and nature needs to exceed the coercive stress. The dependence of coercive stress upon a number of factors such as composition, lattice parameter, and temperature is poorly known but the most important distinguishing feature is that the toughening effect is related to change from one equilibrium state (variant) to another equilibrium state unlike in transformation toughening. The magnitude of the toughening effect is estimated to be $\Delta K_c \sim 2$–$3\ MPa \cdot m^{1/2}$ in yttria -doped zirconia and as high as $\Delta K_c \sim 5$–$7\ MPa \cdot m^{1/2}$ in Ce-doped zirconia, depending upon composition. For the 7 YSZ tetragonal material produced by electron beam deposition, the toughening is rather similar,[19] $\sim 2\ MPa \cdot m^{1/2}$ (Fig. 2) and is produced by switching within individual grains. These values are approximate and there is a clear need for additional work to expand our knowledge of the values of the coercive stress and validate these estimates. In principle, both domain switching and transformation toughening can occur during crack propagation, as has been discussed in greater detail elsewhere.[35]

IV. LTD

Detailed measurements of the kinetics of the moisture-induced transformation of both sintered ceramics and coatings, obtained by either X-ray diffraction[36] or Raman spectroscopy,[37] all indicate that the kinetics can be fit with the standard Mehl–Avrami–Johnson equations for a nucleation and growth process (see Fig. 5):

$$\alpha = 1 - \exp(-(bt)^n) \tag{4}$$

where α is the fraction of tetragonal that has transformed to monoclinic phase, t is the time of exposure to moisture and the value of the constant, b, and the exponent, n, depends on temperature. Experimental data and simulations show that the

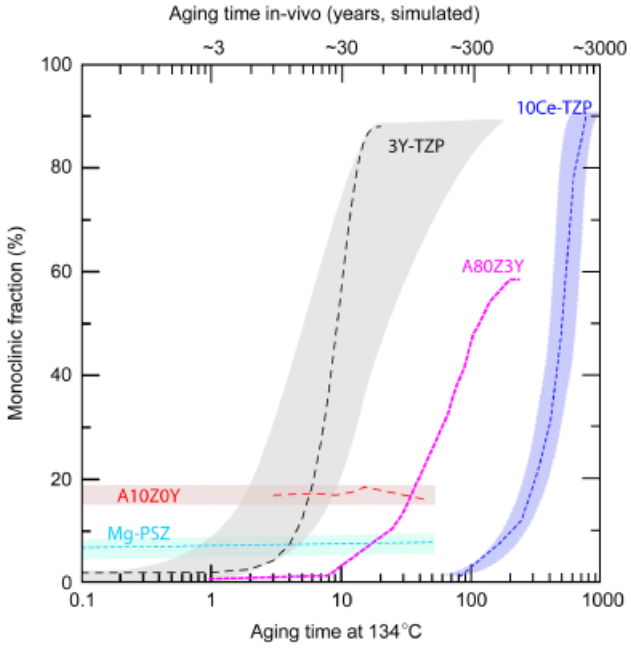

Fig. 5. Low-temperature degradation kinetics of 10 mol% ceria-stabilized zirconia,[39] 3 mol% yttria-stabilized zirconia,[36] Magnesium partially stabilized zirconia,[40] alumina-toughened zirconia (A80Z3Y),[41] and zirconia-toughened alumina (A10Z0Y)[42] measured at 134°C and expected at 37°C (considering an activation energy of 106 kJ/mol for all materials, which is probably not completely accurate). The shadowed areas give uncertainty ranges when they can be evaluated.

exponent has a value between 0.5 and 4.[38] Combining the data obtained at different temperatures, the transformation kinetics form "C"-shaped curves on a time–temperature plot. A number of examples of this time–temperature transformation (TTT) behavior are shown in Fig. 6. At temperatures well below the "nose," the kinetics follow an Arrhenius dependence

$$b = b_0 \exp\left(-\frac{Q}{RT}\right) \tag{5}$$

where b_0 is a constant, Q is an apparent activation energy, R is the gas constant, and T is the absolute temperature. The reported activation energies are close to 100 kJ/mol (~1 eV), a value similar to the activation energy for oxygen vacancy diffusion extrapolated from higher temperatures.

As with other nucleation and growth transformations, the "C"-shaped curve can be interpreted in terms of the competition between the driving forces for nucleation and the growth rates. At low temperatures, below the nose, there is a high nucleation rate and the growth rate is kinetically limited by the growth velocity of the interface between the tetragonal and monoclinic phases. At high temperatures, the nucleation rate is limiting with the driving force for the nucleation of the monoclinic phase being related to the undercooling relative to the T_0 (t/m) temperature. This is also consistent with the observations that the transformation rate decreased rapidly as the T_0 (t/m) temperature was approached, as well as the observation of the reverse monoclinic-to-tetragonal transformation on heating above the T_0 (t/m) temperature.[44]

Microstructural observations of the surface of polycrystalline tetragonal zirconia exposed to water show clearly the nucleation and growth of small regions of monoclinic phase, fully consistent with the MAJ kinetics.[36] Confocal Raman spectroscopy confirms that the transformed regions are indeed monoclinic and, furthermore, that they do not extend deep into the surface, typically less than a few micronmeters before the whole surface is transformed. Careful observations also indicate that there is a preference for nucleation at the grain junctions and corners, and that the transformation then extends across individual grains.[45]

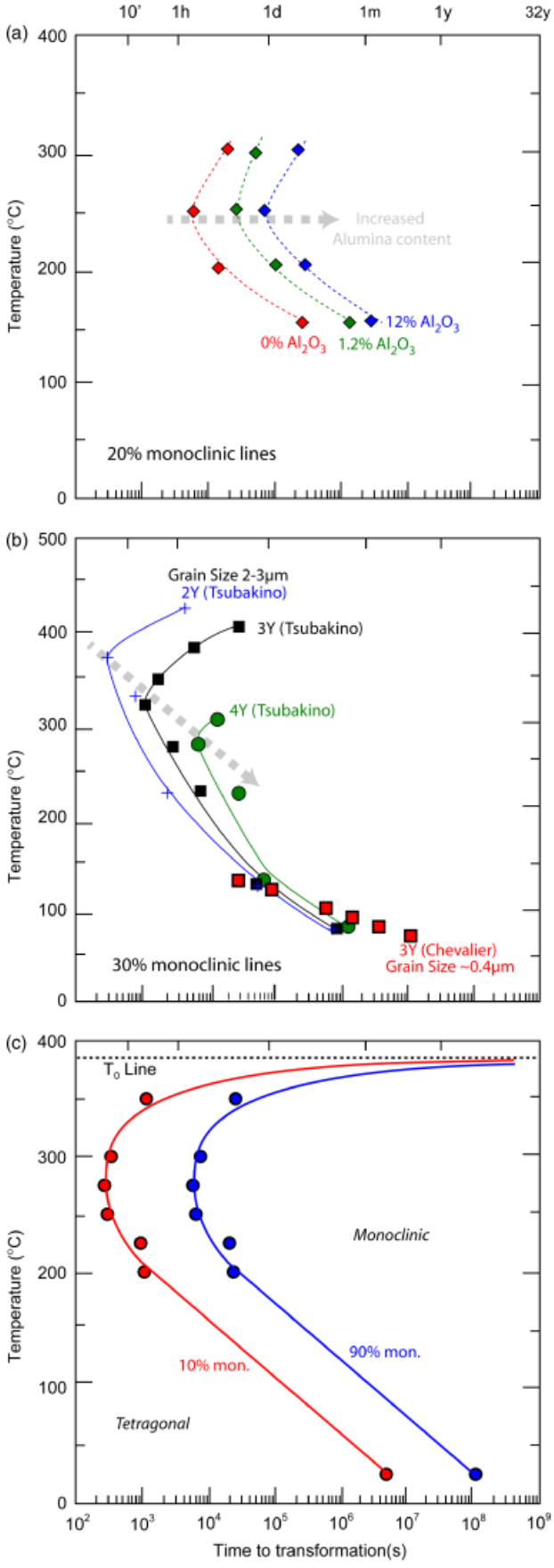

Fig. 6. (a) Time–temperature transformation (TTT) curves of sintered yttria-stabilized zirconia (YSZ) (3 mol% Y_2O_3) and alumina doped YSZ, redrawn from Tsubakino *et al.*[43] (b) TTT curves for YSZ with different yttria-concentrations. (c) TTT curves of 5-YSZ (2.8 mol% Y_2O_3) thermal barrier coating.[44]

The connection between the presence of moisture and the degradation of polycrystalline tetragonal ceramics remains to be firmly established. Indeed, some authors claim that exposure to moisture increases lattice parameters of the tetragonal phase[46] while others claim that lattice parameters decrease under the same conditions.[47] The filling of oxygen vacancies by "water-derived species" (often proposed to be hydroxyl ions) probably leads to both decrease of ΔG_c (by modifying the local oxygen configuration around Zr ions) and an alteration in internal stresses in the grains in contact with water. Further, more detailed experimental work and computational atomic scale simulations are necessary to resolve this crucial issue of the nature of the diffusing species. Based on the superposition that exposure to moisture leads hydroxyl ions to diffuse into the lattice by an oxygen vacancy diffusion mechanism,[47] the role of moisture can be understood as follows and as shown schematically in Fig. 7. Inward diffusion of a moisture species generates tensile hydrostatic stresses in the grains (with the maximum stresses in those grains roughly estimated to 300–500 MPa by Shubert and Frey[47]) and modifies the oxygen configuration around the Zr ions, both of which may lead to destabilization of the tetragonal phase. The tensile stresses are expected to be largest at grain junctions and edges, favoring nucleation of the transformation at these locations, as is indeed observed. The volume increase of the transformation produces a surface uplift related to the detailed crystallography as described in Panel B. The large shear strains and displacements accompanying the transformation can also create cracks along the grain boundaries[48] that in turn allow the moisture to penetrate further into the material and the process is repeated as moisture ingress continues. As it is likely that the moisture can flow through grain boundary cracks much faster than by diffusion, it is likely that the observed activation energy for LTD is determined by diffusion of the moisture species in the lattice of the individual grains. "Section VII" will discuss the major unresolved issues on the underlying mechanism by which moisture facilitates the transformation from tetragonal to monoclinic zirconia.

Much less is known about the behavior of the metastable tetragonal-prime zirconia phase when exposed to typical conditions under which LTD occurs in sintered material of the same composition. As described in the previous section, tetragonal-prime zirconia can be formed by either of two methods: (i) heating to a sufficiently high temperature where the cubic phase is the equilibrium phase and then cooling, or (ii) directly by rapid deposition from the vapor or liquid. The low-temperature aging of the former has been studied by Jue *et al.*,[49] who found that the resistance to low-temperature transformation of the 3 YSZ composition was significantly greater than the same composition formed by conventional sintering. They also found that the resistance to LTD depended on the microstructure: material with small domains being most resistant and those materials with larger domains being less so. The tetragonal-prime zirconia, of similar composition, but produced by high-rate deposition, as exemplified by 8 YSZ TBCs is also highly resistant to LTD. Only after prolonged high-temperature annealing, during which it phase separates into a mixture of tetragonal and cubic phases, does the transformation occur.[50] Even then, it appears that a critical size of the tetragonal grains has to be attained before transformation is appreciable.

V. Current Applications of Zirconia and Impact of $t-m$ Transformation

(1) Body Implants

Biomedical implants are increasingly being used to restore a body function that has been deteriorated by a disease or a trauma. In addition to being biocompatible and chemically inert for tens of years *in vivo*, both mandatory requirements, a ceramic implant has to resist wear and cyclic fatigue for several millions cycles under high loads. In the 1990s, zirconia was introduced in orthopedics as an alternative to alumina because of its higher fracture toughness.[51] Since then around 600 000 zirconia femoral heads have been implanted. Ca- and Mg-stabilized zirconia were the first to be proposed for this application, but based mainly on higher strength at room temperature 3 *m/o* Y_2O_3 (3Y-TZP)-stabilized zirconia soon became the material of clinical choice. Its use also made possible the design of smaller hip implants (such as the 22.22 mm diameter femoral heads) and knee joints that did not have adequate reliability when made with alumina. Clinical results reported before 2000 were satisfactory, with especially low failure rates reported for zirconia femoral heads. However, in 1997 the U.S. Food and Drug Administration (FDA) first reported that the standard steam sterilization procedure (134°C, 2 bars) led to surface roughening of temporal head implants. More importantly, in 2001, the FDA announced that firms distributing zirconia were recalling femoral heads owing to a series of fractures. The origin of failures was related to an accelerated LTD of zirconia in a limited number of batches of implants.[52] This fracture episode has had a strong negative impact on the use of zirconia in orthopedics. In particular, the main supplier of zirconia implants at that time, Saint Gobain Desmarquest, stopped manufacturing biomedical devices and other companies, such as Ceramtec in Germany, switched to using YSZ in alumina-zirconia composites. Since then, it has been estimated that more than 250 000 alumina–zirconia (Biolox Delta®) femoral heads and 150 000 acetabular cups have been implanted in the last 5 years.

The failure episode of 2001 emphasized the critical role of LTD on zirconia implants. Several clinical studies and retrieval analyses were then devoted to zirconia implants. They showed that even zirconia implants processed under the best conditions could suffer from a certain degree of degradation *in vivo*. Depending on the retrieval analysis used, the extent of degradation ranged from roughening (due to surface uplifts), hardness decreases (due to microcracking) to failure (slow crack growth). The reader may refer to Chevalier *et al.*[50] for a detailed review of retrieval and clinical analysis. Most of the clinical studies showed a significant increase in the overall wear rate of hip prostheses related to the use of zirconia femoral heads. The increase in wear rate only became evident after several years and was related to a large degree of $t-m$ surface transformation of the heads associated with altered roughness and sphericity. This results in billions of sub-micrometer-sized wear debris being shed into the surrounding synovial fluid and tissues. The biological interaction with small particles in the body then becomes critical: wear particles generated at the contact surfaces enter the periprosthetic tissues where they trigger macrophage reaction. Then macrophages release pro-inflammatory cytokines that stimulate osteoclastic bone resorption, leading to osteolysis and eventual loosening of the prosthesis and a need for replacement of the implant. It is not clear today if wear and aging are synergetic effects, although we might reasonably expect so.

(2) Dental Applications

In the late 1990s, the success of zirconia in orthopedic implants at that time encouraged its development for dental restoration components such as crowns and bridges. In contrast to the switch to two-phase zirconia composites adopted by the orthopedic companies, monolithic 3Y-TZP is increasingly being used today in dental applications.[53] In part this is because zirconia can be readily tinted by doping to match existing teeth in color but it is surprising, nonetheless Because the material can be expected to be as susceptible to LTD as in orthopedic applications, even though the temperatures are somewhat lower. Although the consequences of failure of a dental implant or dental restoration device is less critical to a patient than that of an orthopedic implant, the durability of these dental devices is expected to be no less of an issue for their manufacturers.

(3) Zirconia Electrolytes

One of the major applications of YSZ is as an ionic electrolyte in solid oxide fuel cells (SOFC) and sensors, such as oxygen

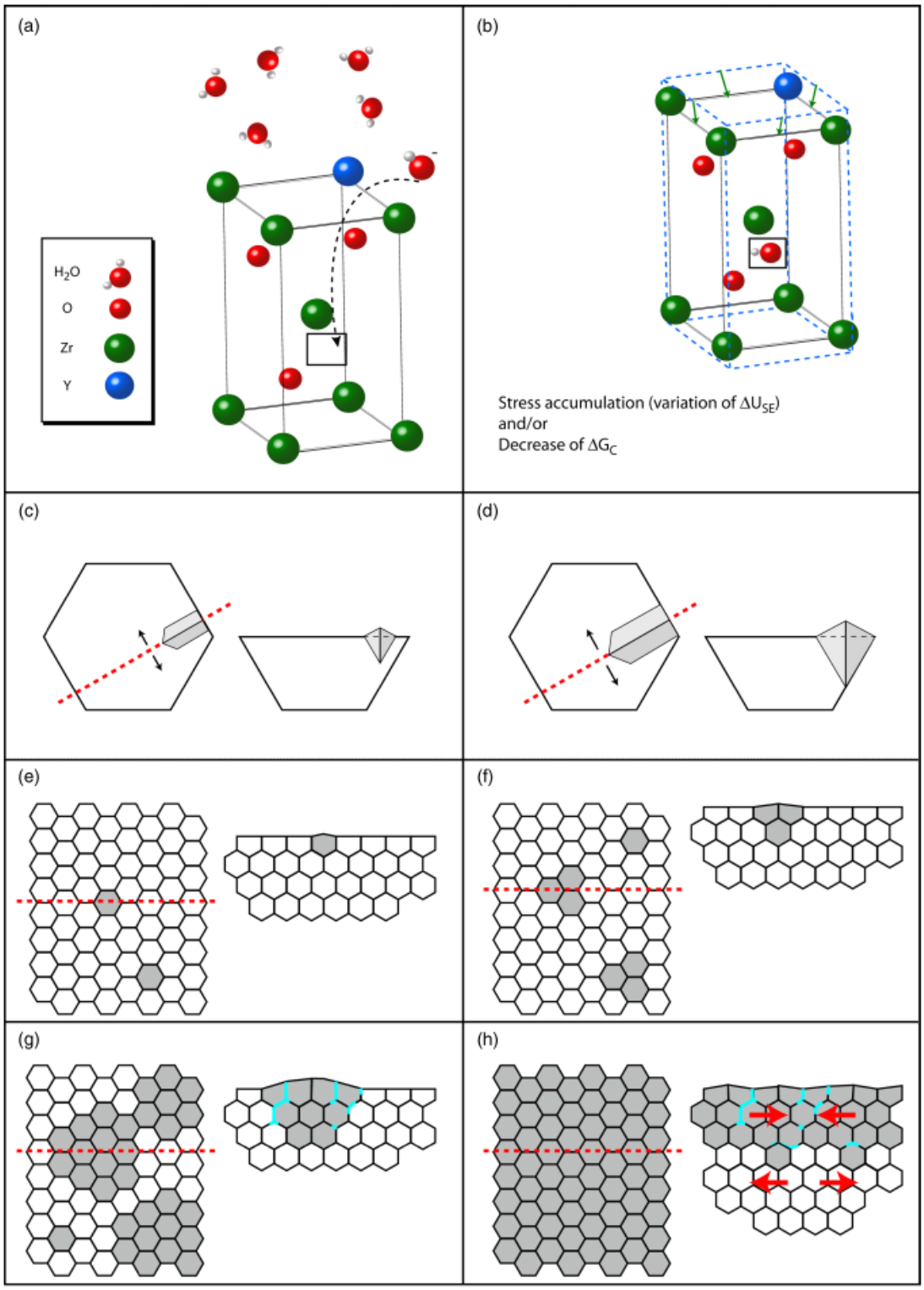

Fig. 7. The steps of the low-temperature degradation process: from chemical interactions towards surface uplifts and microcracking. (a) Diffusion of water species (here OH^-) into the lattice via oxygen vacancies and (b) resulting change of lattice parameters. (c) Nucleation and (d) growth of monoclinic phase (in grey) from grain boundary to the interior of one grain (top view on the left, and cross section on the right). (e)–(g) Nucleation and growth at the microscale: simultaneous apparition of new monoclinic nuclei and extension of the existing ones (top view on the left, and cross section on the right). The transformed zones are protruding from the surface. For a given surface monoclinic content, microcracks (in blue) are formed. (h) Surface entirely transformed: the transformation then proceeds to the bulk because water can penetrate through microcracks network and underlying tetragonal grains are in tension (arrows indicate the nature of the stress).

sensors. In the majority of instances, the zirconia is used in its cubic form and at high temperatures to maximize the ionic conductivity. Under such operating conditions, both the temperatures are sufficiently high (typically above 600°C and hence above T_0 (t/m)) and the yttria concentration sufficiently high, typically 9 m/o Y_2O_3, that transformation and degradation is not anticipated to be a problem. This is borne out even for SOFCs in which water is generated as a result of the electrochemical reaction. There are two accounts in the literature that indicate that transformation to the monoclinic phase can occur under an applied voltage at the anode of YSZ. However, although these observations may provide additional insight into the mechanism of transformation, they are not indications of LTD in zirconia fuel cells even though the geometry is the

same as a fuel cell. In the case of the work by Badwal and Nardella,[54] they applied an external voltage to a 3 *m*/*o* Y_2O_3 electrolyte cell rather than operating the cell under an oxygen potential gradient and furthermore the applied voltage was in excess of the decomposition potential for zirconia (which is ~2 V). As a result, the electrochemical conditions were very different from those of a fuel cell. Interesting, they only observed the transformation at a temperature below the T_0 (*t*/*m*) and when they repeated the test at a higher temperature they saw no transformation. The other account[55] of degradation was also in a similar cell geometry with an external voltage applied across a co-doped yttria, Nb-stabilized zirconia. Again, the conditions employed were not representative of a SOFC but do provide valuable insights. These will be discussed later.

There are two developments in zirconia-based fuel cells where degradation may occur under rather restrictive conditions. One is the use of zirconia with lower concentrations of yttria, motivated by their superior fracture toughness. Although the highest ionic conductivity is exhibited by cubic YSZ close to the 9 *m*/*o* Y_2O_3, its inferior fracture toughness (Fig. 2) has led some organizations to investigate the tetragonal 7.6 *m*/*o* $YO_{1.5}$ (YSZ) zirconia as an alternative electrolyte composition. These compositions are metastable with respect to phase separation into a mixture of tetragonal and cubic phases and so whether they are susceptible to transformation will depend on whether the operating temperature of the fuel cell is above or below the T_0 (*t*/*m*) temperature for the chosen yttria concentration. A similar situation arises in the development of thinner zirconia electrolytes produced by deposition processes, such as sputtering. Thinner electrolytes have lower impedance and consequently offer the prospect of lower cell operating temperatures and reduced problems associated with metal electrode oxidation. Indeed, recent results have shown that the peak ionic conductivity occurs in thin sputtered zirconia films at yttria concentrations of ~6.5 *m*/*o* Y_2O_3 rather than the ~9 *m*/*o* Y_2O_3 of bulk zirconia electrolytes.[56] As with the other developments, the issue is whether the operating temperature is below the pertinent T_0 (*t*/*m*) temperature.

(4) TBCs

The primary function of a TBC is to provide thermal protection to metallic engine components in a thermal gradient enabling them to be used in the presence of hotter gases than they could otherwise be exposed to for prolonged periods of time. The majority of applications involves the protection of gas turbine blades, vanes, and combustors for both aerospace and power generation turbines but they are also being used in the cylinders of diesel engines and other situations where high-temperature insulation is required. The use of TBCs has already facilitated the increase in turbine inlet temperatures as well as improvements in fuel efficiency.[57,58]

The initial selection of zirconia as a TBC was based on three considerations: its high melting temperature (2700°C); its exceptionally low thermal conductivity[59] (~2 W/mK) and the fact that it could be plasma sprayed on complex shapes, such as blades. The subsequent identification of 8 YSZ (7.6 *m*/*o* $YO_{1.5}$) as the composition of choice was made soon after TBCs were first introduced into gas turbine jet engines. Several different compositions, including Mg- and Ca-stabilized zirconias, which were then being widely used in industry, were investigated. However, work at NASA Glenn (then NASA Lewis) by Stecura[60] showed that coatings of the 8 YSZ composition exhibited the longest thermal cycle life. Recent work has demonstrated that this metastable composition has the highest fracture toughness and is probably a result of ferroelastic toughening.[61] Since its first use in jet engines, the use of zirconia coatings has enabled turbines temperatures to be increased substantially with commensurate increases in efficiency and power.

Several attempts have been made to produce TBCs of both higher yttria concentrations, because they have lower thermal conductivity,[62] and lower yttria concentration. The former have generally been unsuccessful because their fracture toughness is significantly lower than 8 YSZ and the latter because of their susceptibility to LTD.

A feature of the 8 YSZ TBCs, whether deposited by plasma spraying or electron beam physical vapor deposition, is that they consist of the metastable tetragonal-prime phase. This is because both deposition methods are high rate processes. At high temperatures, the metastable composition slowly separates into a mixture of tetragonal and cubic phases having equilibrium compositions dependent on the temperature as depicted in Panel A and with kinetics also dependent on the temperature. Under current turbine use conditions, this phase separation is believed not to be complete and no transformation to monoclinic occurs. (Some plasma-sprayed coatings are reported to contain some monoclinic phase but these are in the as-deposited coatings suggesting that the starting powder was inhomogeneous.) However, as the engine temperatures are increased in pursuit of higher energy efficiency, there will be conditions of temperature and service at which the transformation may occur. Studies of the behavior of 5 YSZ and 8 YSZ TBCs after prolonged high temperatures indicate that phase separation into equilibrium mixtures of tetragonal and cubic phases occurs, for instance after 350 h at 1425°C, and that these can be cooled to room temperature without transformation to monoclinic.[37] However, if the coatings are subsequently held at intermediate temperatures in air, a portion transforms to monoclinic.[37,44] The kinetics of the transformation (Figs. 5 and 6) are consistent with those reported for the LTD of sintered ceramics. Furthermore, but not shown in the figure, there appears to be a correlation between the size of the tetragonal regions and their susceptibility to transformation but this needs further clarification.

Two recent developments in turbine operation may impact the susceptibility of current TBCs to LTD. One is the increasing use of steam injection in the combustion process, a process introduced to both increase output power and decrease engine exhaust NO*x* pollution. The other is the frequent washing of engines with high-pressure steam to clean away dirt and residues that can adversely affect engine efficiency.

VI. Lessons Learned and Future Developments

(1) Lessons Learned

As described previously, the isothermal *t*–*m* transformation of zirconia leads to surface uplifts and potential microcracking. Both features can have direct effects on the degradation of zirconia devices functionality. For instance, surface uplift and microcracking may impact wear properties, through roughening and grain pull-out. In the most severe cases, microcracking may induce slow crack growth and delayed failure.

(A) Porosity Distribution and Control: The implications of aging on biomedical implants have been reviewed previously and are not repeated here.[50] However, analysis of the failure of zirconia femoral implants has provided considerable insight into the importance of microstructural and compositional control in affecting the susceptibility to LTD. This is in addition to the well-established dependence of degradation on grain size and yttria composition. One of the intriguing observations of LTD in zirconia implants was the apparent variability from one femoral head to another that are now understood to be the result of microstructural and compositional variations.

The failures of these zirconia femoral heads have been widely discussed in the past 5 years, but no comprehensive view has previously been published, in part because of confidentiality issues. We try to put together the pieces of the puzzle in Fig. 8. It transpires that the femoral heads that broke were all sintered in a new tunnel furnace rather than in batch furnaces as was previously done. This modified the pore distribution inside the balls, without changing significantly measured average-sintered densities. (Internal quality procedures required the average density of each ball to be above 6.08 g/cm^3 (99.6% of theoretical density), while ISO standards only required a lower density of

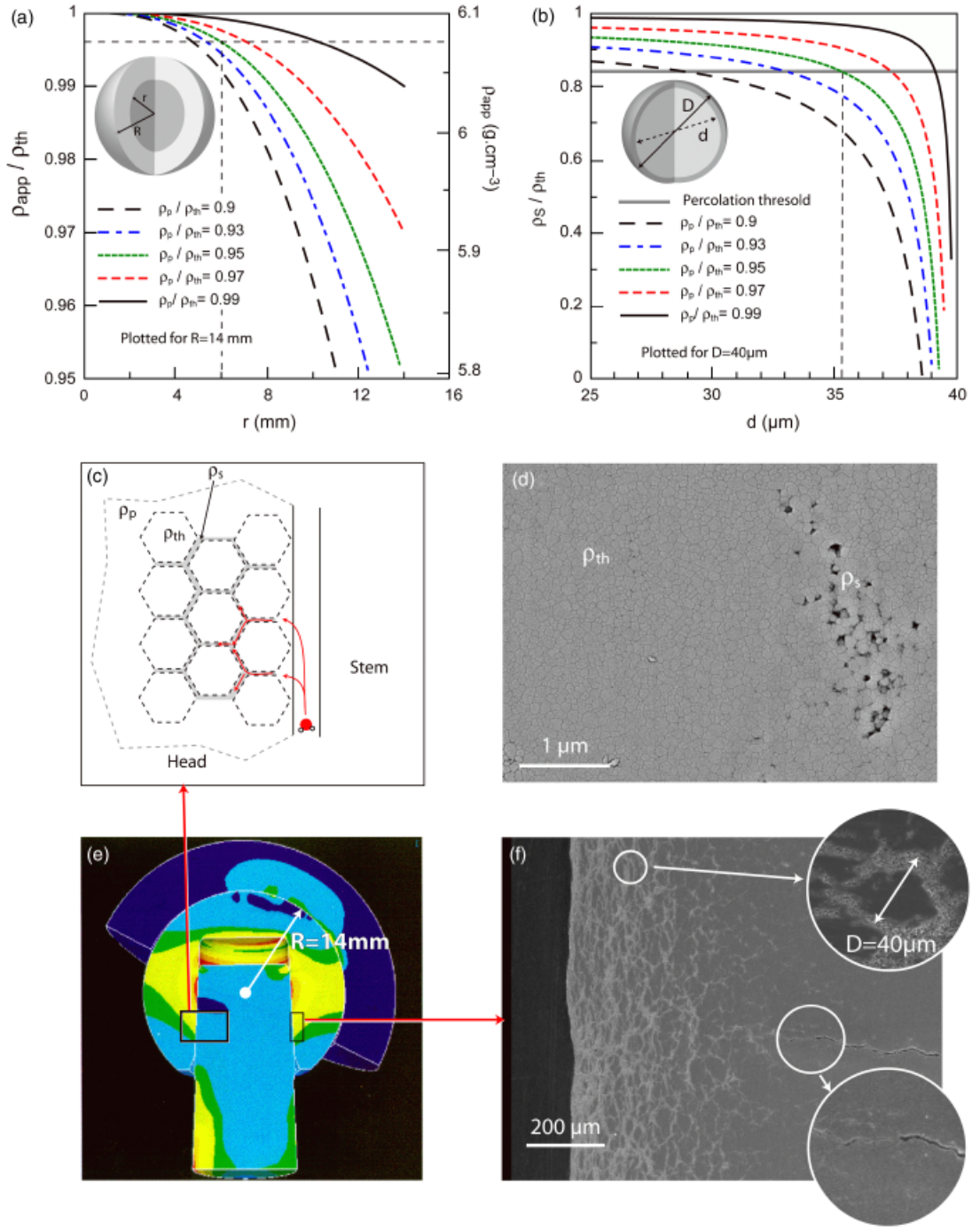

Fig. 8. Possible scenario of the origin and mechanisms of Prozyr® heads failures. (a) Variation of the apparent density of a zirconia ball (ρ_{app}) with the radius of a porous core of density ρ_p. (b) Density of the porous shell (ρ_s) around a granule versus the diameter (d) of the dense part of the granule, for a given average density ρ_p. (c) Schematic access of water in the porous core of the head following the interface with the stem, and penetrating through the percolating porosity. (d) SEM observation of the porosity in the Prozyr® zirconia heads near the center of the balls, justifying the core-shell description of the porosity. (e) Finite element analysis of the stresses in a hip joint head, showing large stresses (in red) at the interface with the metallic taper, unfortunately located near the most porous region of the head in contact with body fluids. (f) SEM cross section taken in the region of interest after *in vivo* aging (<2 years) showing 5-μm-thick transformed zones around granules (upper inset), leading to a percolating transformed network 500 μm deep. Lower inset shows the crack initiation induced by the large transformed zone.

6.0 g/cm^3.) The balls were formed by cold isostatic pressing of spray-dried powder, which associated to fast sintering, introduces porosity at two different scales: at the scale of the ball (the core being more porous than the surface) and at the scale of the spray-dried granules (the surface being more porous than the core). The results are shown in Figs. 8(a) and (b) for different porous core and granule diameters. The relatively small changes in density associated with this type of porosity were undetectable by the quality control methods then in place. After sintering, balls were machined to the final shape. Following machining, the percolating porosity gained an access to a free surface in potential contact (even if indirect) with body fluids as illustrated in Figs. 8(c) and (e). Analysis of the balls revealed that after sintering, the balls sintered in the tunnel furnace contained interconnected porosity along the periphery of the original granules, which, it is presumed, allowed percolative transport of moisture deep into the balls accelerating their LTD. Finite element computations further indicate that the regions where the degradation was fastest correlated with the regions of the highest tensile stresses. Microstructural characterization of degraded balls provided clear evidence for the presence of thick transformed zones along the boundaries of the granules as well as a

network of zones percolating deep into the balls as shown in Fig. 8(f).

Insight into the effect of porosity at different length scales can be obtained from a simple core-shell model. Assuming that the shell is less porous, one may calculate the apparent density of a spherical ball, ρ_{app}, in terms of its radius, R, vs the radius of a porous core, r, of given density ρ_p

$$\rho_{app} = \rho_{th} - \left(\frac{r}{R}\right)^3 \times (\rho_{th} - \rho_p) \quad (6)$$

where ρ_{th} is the theoretical density of a tetragonal 3Y-TZP (6.1 g/cm^3). For example, for a typical, standard sized 28 mm ball of apparent density 99.6% may contain a core of radius 5 mm and average density 95%. In this porous core, the granules may also be represented by a core-shell model. For a granule of diameter D and average density ρ_p, which contains a fully dense core of diameter d, the density ρ_s of the porous shell is given by

$$\frac{\rho_s}{\rho_{th}} = \frac{D^3(\rho_p/\rho_{th}) - d^3}{D^3 - d^3} \quad (7)$$

Figure 8 represents this model for granules of diameter $D = 40$ μm, which corresponds to the average size of spray-dried granules used for the process of Prozyr® balls. Taking the example of a 28 mm ball ($R = 14$ mm) of apparent density $\rho_{app} = 99.6\%$ containing a core of radius $r = 5$ mm and density $\rho_p = 95\%$, percolation of the porosity may occur if the porosity is localized in a 5-μm-thick layer around each granule (meaning that in this layer the porosity reaches 16%).

(B) Phase Separation (Stabilizer Partitioning): A second factor influencing certain *in vivo* implant failures was found to be the presence of the cubic phase. This occurred for products sintered at high temperatures, above 1500°C and for several hours (see comments on yttrium diffusion in Panel A) and applied to some femoral heads produced in the past. The degradation was attributed to the formation of locally depleted tetragonal grains in the vicinity of the cubic grains.[14] As indicated in Panel A, the significance of the phase partitioning into yttrium-rich cubic and yttrium-poor tetragonal phases is that the yttria-depleted tetragonal grains are less stable to transformation and act as preferential nucleation sites for the t–m transformation.

In general, phase separation can be expected to occur for all compositions sintered or deposited in two-phase regions of the phase diagram. The kinetics of the phase separation are associated with the partitioning of the stabilizer ion which, in turn, depend on the stabilizer diffusion coefficient in zirconia and the free energy difference between the metastable phase and the equilibrium phases at the sintering or annealing temperature. For this reason, the driving forces for phase separation are distinct from the driving forces for the LTD. Similarly, the kinetics is quite different, the phase separation being controlled by cation diffusion whereas the degradation itself is controlled by anion diffusion.

(C) Effect of Machining: The role of grinding to shape and subsequent polishing following sintering is not yet completely understood. One effect is to remove surface layers and expose interconnected porosity. The effect of residual stresses introduced by grinding is more subtle. On flat surfaces, grinding usually produces surface compressive stresses. Indeed, this has been investigated as a general means of increasing the strength of zirconia-containing materials.[3] Such compressive stresses are expected to be beneficial in increasing the aging resistance. However, the polishing that follows can then be critical, if it removes portions of the compressive surface layer. The scratches may also induce local residual tensile stresses and act as nucleation sites for LTD (the propensity for nucleation of the monoclinic phase on scratches is shown in Figs. 2 and 3 of Deville *et al.*[63]). Rather than the roughness *per se*, it appears that it is the surface residual stress state that governs nucleation of the transformation at the surface.[63] So polishing may remove the compressive layer introduced by grinding but leave a large density of scratches that can dramatically increase the degradation rate. Consequently, careful polishing is needed to achieve good aging resistance. In the case of most of commercial ceramic implants today the roughness of the bearing surfaces is controlled to <5 nm root mean squared (R_q parameter).

Other work has shown that the effect of grinding and polishing can be more complex and a complete understanding remains to be established beyond the concepts discussed in the previous paragraph. For instance, Whalen *et al.*[64] have shown that LTD of a 2.45 *m/o* Y_2O_3-sintered material could be inhibited by first grinding the surface and then subsequently annealing above 1200°C. This was attributed to the reverse transformation, during annealing, of the monoclinic phase formed by grinding. Similarly, Jue and colleagues[49,65] report that samples of tetragonal zirconia that were ground were also more resistant to LTD. They attributed this improvement to decreasing the size of the ferroelastic domains. This hypothesis was supported by experiments on tetragonal-prime zirconia (which contains very small domains): upon surface grinding, some of the domains re-oriented, effectively increasing the domain size and leading to increased LTD kinetics.

(D) Postsintering Processing: One of the unexpected surprises encountered early in the development of femoral heads was the poorer behavior of those that had been hipped (HIP) after sintering. The hipping step was introduced to close up remaining porosity but these heads, which were not re-oxidized after HIP and remained black in color, were implanted in the 90s but exhibited very poor behavior: in a large-scale clinical study,[66] the failure rate due to aseptic loosening after 8 years reached 37% while it was limited to 4% with alumina. Because of these unexpectedly poor results, zirconia heads were then systematically reoxidized after HIP. Subsequent laboratory autoclave testing confirmed that the zirconia reduced by annealing in an argon/hydrogen atmosphere for 30 min at 1400°C indeed underwent faster transformation to monoclinic.[67] It is tempting to interpret the higher transformation rate to the higher concentration of oxygen vacancies introduced by the reduction process. However, the concentration of vacancies introduced by reduction is orders of magnitude smaller than the concentration introduced to charge compensate for the yttria stabilizer, and hence is unlikely to be responsible for the higher transformation rate. More likely, reduction increases the electron concentration and, in turn, the hydrogen transport and H_2O permeation.[68]

(E) Life Prediction: A requirement of any biomedical implant is that it be sterilized before surgical implant. One of the common sterilization methods is steam exposure at 134° or 140°C for <1 hour. As mentioned earlier, in 1997 the U.S. Food and Drug Administration (FDA) reported that steam sterilization led to surface roughening of zirconia implants, and it and other regulatory authorities over the world then advised against autoclaving zirconia implants.[69] These actions led to a variety of attempts to simulate aging *in vivo* and use the results for life prediction. The studies highlighted the difficulty of life prediction of LTD based on accelerated testing at different temperatures. In the context of the TTT curves, robust prediction based on the kinetics is really only possible when the accelerated testing is carried out well below the nose temperature, especially when extrapolating to low temperatures, such as body temperatures. The predicted *in vivo* aging kinetics shown in Fig. 5 are based on extrapolations based on Eqs. (4) and (5) using an activation energy of 106 kJ/mol.

(2) Alternative Zirconia-Based Materials

(A) Ceria-Doped Zirconia: Other than YSZ, the ceria-stabilized system has probably been studied in the most detail. Ceria-doped zirconia has been reported to exhibit substantially reduced susceptibility to LTD[39,70] (Fig. 5). In large part this is understandable from the metastable phase diagram shown

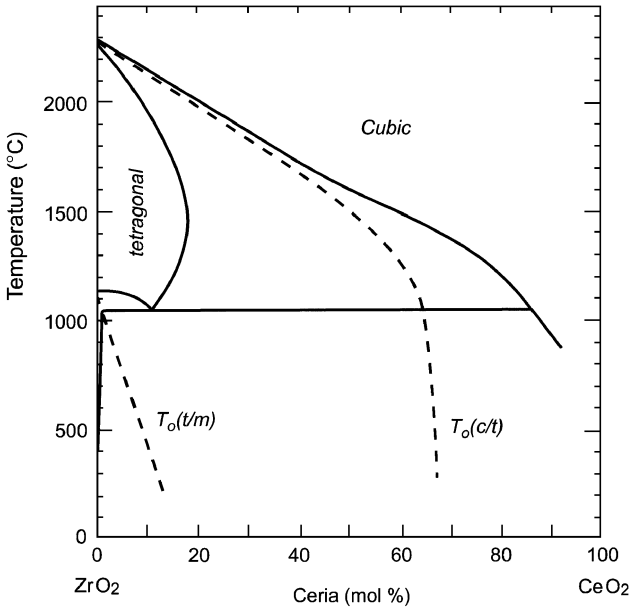

Fig. 9. Zirconia–ceria phase diagram, redrawn from Yashima *et al.*[5]

in Fig. 9, redrawn after Yashima *et al.*[12] According to this diagram, the T_0 (t/m) line falls to zero at $\sim$16 m/o CeO_2, a composition lower than the maximum solubility of CeO_2 in tetragonal zirconia at 1400°C. Figure 5 shows the $t-m$ transformation kinetics of a zirconia stabilized by 10 m/o CeO_2 (10Ce-TZP) aged at 134°C, 2 bars.[39] According to the phase diagram the material is fully tetragonal at the sintering temperature and on cooling becomes metastable with respect to the formation of monoclinic at a T_0 (t/m) temperature of $\sim$400°C. However, as indicated by the aging resistance curves in Fig. 5, this composition is far more resistant to LTD than the corresponding YSZ compositions. The comparison is especially pertinent because both 10 m/o CeO_2 and the 3 m/o Y_2O_3 have almost the same T_0 (t/m) temperature, implying that the driving force for the $t-m$ transformation is almost the same.

Ceria-stabilized zirconia also differs from YSZ in that no vacancies are required to charge compensate for the ceria stabilizer, at least in the Ce^{4+} state. As the mechanism for LTD has been attributed to oxygen vacancy annihilation by in-diffusion of OH^- ions, it is tempting to interpret the resistance to degradation of the ceria materials to the lack of oxygen vacancies. However, this then raises the question as to why the ceria-stabilized zirconias transform at all. The kinetics of the degradation are very slow and as indicated in Fig. 5 for both the 10 and 12 Ce-TZP materials, the extrapolated lifetimes at body temperatures far exceeds human life expectancies. This suggests that the single-phase ceria-stabilized zirconia are to be preferred for applications, such as biomedical implants, where resistance to LTD is crucial. A further advantage is that with appropriate processing, the fracture toughness of the 10 and 12Ce-TZP materials is comparable with that of 3Y-TZP.[39] It is also notable that as with the YSZs, increasing the concentration of ceria makes the zirconia even more resistant to LTD. This has recently been shown in comparison of 10 m/o CeO_2 and 12 m/o CeO_2 (12Ce-TZP) in unpublished results by El-Attaoui.[39]

One possible explanation for degradation even in the absence of charge compensating vacancies is that the native oxygen vacancies, those present for thermodynamic equilibrium at the sintering temperature, are retained and are responsible for mediating the inward diffusion of moisture species. The concentration of these native vacancies is much lower, being determined by the oxygen vacancy formation energy, than the concentration of charge compensating vacancies in the trivalently stabilized zirconias. Another possibility that has yet to be explored in detail is that there is a finite concentration of Ce^{3+} ions in the zirconia.[71]

(B) Other Stabilizers and Compositions: Until a comprehensive and detailed mechanism is identified for LTD, the appropriate choice of dopant remains largely a matter of experimentation. One requirement for increased resistance to LTD is that composition be chosen so that the T_0 (t/m) temperature is as low as possible so that, in turn, the kinetics, are as slow. This favors two-phase zirconia compositions, for instance as in the yttria-stabilized system where the lowest yttria concentration is given by the t/c boundary line, rather than single-phase zirconia compositions. Thus, in the Scandia-stabilized zirconia system, the T_0 (t/m) temperature for the 8 m/o $ScO_{1.5}$ composition, the limit of the tetragonal field is $\sim$320°C, whereas in the erbium-stabilized zirconia system the T_0 (t/m) temperature of the corresponding limiting composition is closer to 650°C. Ideally, T_0 (t/m) temperature corresponding to the solubility limit for the tetragonal phase at the sintering temperature would be below room temperature as it is for the ceria system. In addition, based on the role of the Fermi level in dictating the solubility of mobile charge species, it is likely that the higher the stabilizer concentration the better. However, although such approach to decrease the T_0 (t/m) temperature is appealing to decrease LTD at room temperature, it also leads to decrease in the propensity of zirconia to transform under stress. Thus, zirconia with a too low T_0 (t/m) temperature will exhibit poor toughness, or at least poor transformation toughening ability. Therefore, any choice of a new alloy will be confronted to a challenge: decreasing the LTD sensitivity without decreasing too much the T_0 (t/m) line.

As was evidenced by the comparison between 10Ce-TZP and 3Y-TZP, materials with the same driving force for LTD (same T_0 (t/m) temperature) can exhibit very different LTD kinetics. Therefore improving the LTD–toughness balance may be achieved by keeping the T_0 (t/m) temperature high enough and decreasing the kinetics of the process controlling LTD (i.e., water-derived species diffusion and/or oxygen vacancy diffusion). It is possible that zirconias doped with more than one stabilizer offer such balance. The metastable phase diagrams are not known for codoped zirconias but if it is assumed that the kinetics are dictated by the concentration of vacancies, then one approach to selecting codopants is to combine trivalent and pentavalent ions to minimize the total concentration of vacancies required for charge compensation. This may have been the basis for the investigation of yttria–niobia codoped zirconia by Kim *et al.*[55] although they did not use the equimolar mixture of the two stabilizers required to maintain a single-phase tetragonal composition. An alternative composition worthy of investigation would be equimolar yttria–tantala tetragonal zirconia. Compositions in this region also exhibit unusually high fracture toughness without any apparent stress-induced transformation.[72]

(C) Two Phase Zirconia Composites: There are several reports that alumina–zirconia composites (Al_2O_3–YSZ) have significantly slower transformation kinetics than zirconia alone,[41,43] and as mentioned a two-phase alumina–zirconia material is currently being marketed for orthopedic applications. The retardation afforded by adding minor amounts of alumina is illustrated by the comparison (Fig. 6) between the TTT curves for 3 mol% Y_2O_3 and the same zirconia with different (low) concentrations of alumina.[43] Also, as shown in Fig. 5, alumina containing a small concentration of zirconia is also exceptionally resistant to LTD. In discussing these observations, it is useful to distinguish between these two types of composites depending on the majority phase.

There is as yet no completely satisfying explanation for the slower LTD kinetics in zirconia containing small concentrations of alumina. What is clear is that residual stresses due to thermal expansion mismatch between the alumina and zirconia cannot account for the good LTD resistance, because the zirconia phase in the bulk will be under net hydrostatic tension and at the surfaces under approximately biaxial tension. A hydrostatic tensile stress in the tetragonal zirconia decreases the elastic constraint on the tetragonal phase and should favor its transformation to monoclinic. The residual stress created by the

thermal expansion mismatch can be quite large, depending on the volume fraction.[73] However, for the two alumina composites studied by Tsubakino *et al.*,[43] the residual stress in the zirconia is estimated from Ma *et al.*[73] to be only 8 MPa and 60 MPa for the 1.2 and 12 vol% compositions, respectively. It is also difficult to believe that small amounts of alumina appreciably increase the elastic stiffness of the material and thereby increase the elastic strain energy associated with the transformation of particles. Other factors that might affect the resistance to aging have not yet been investigated in the detail necessary to clarify the increased resistance to aging. For instance, the grain size and silica impurity content at grain boundaries are both affected by the addition of alumina. Typically, the addition of small volume fractions of alumina reduces the grain size of zirconia.[41] Also, alumina getters silica impurities at the grain boundaries, a phenomenon discovered by combined ac impedance and transmission electron microscopy studies of YSZ. It can be anticipated that the diffusion of moisture species is slower in the absence of a silica grain boundary phase, especially along the three-grain junctions that are continuous in microstructures. One striking feature of the TTT data in the Fig. 6 is that neither the activation energies for the degradation nor the "nose" temperature are greatly affected by the volume fraction of alumina added. This suggests that the driving force for the transformation given by the T_0 (t/m) temperature for the zirconia in these materials and the diffusion mechanism associated with the transformation have not been altered. Rather, the systematic shift in the TTT curves to longer times in Fig. 6 is indicative of a decrease in area fraction of zirconia exposed to the moisture environment as the alumina fraction is increased.

The explanation for the retarded kinetics is perhaps clearer in the materials in which alumina is the major phase[42] (sometimes referred to as zirconia-toughened alumina, or ZTA). Historically, contrary to the name, zirconia was added to increase the strength of alumina by limiting grain growth. Two distinct classes of retardation contributions can be considered. The first is simply topological: if the zirconia phase is not microstructurally continuous, then there is not a pathway for diffusion of the moisture species into the ceramic and so the degradation cannot continue past the surface and deep into the material. The necessity of a percolative pathway has been underscored by experiments in which alumina and 3Y-TZP mixtures of different volume fractions were subject to steam sterilization. As shown by the results in Fig. 10, transformation to monoclinic occurs once the percolation threshold is exceeded.[74] (For random distributions of spheres, the percolation threshold is $\sim$16 volume fraction.[75])

The second contribution is related to the metastability of the tetragonal phase of the zirconia discussed in the previous section. Even if zirconia grains in ZTA are likely to be in net tensile stress after processing as a result of thermal expansion mismatch, the transformation is hindered by the much stiffer alumina matrix. This can be appreciated from Eq. (1): the elastic self-energy ΔU_{SE} term is directly related to the modulus of the surrounding matrix, so a stiffer material matrix, such as alumina, increases ΔU_{SE}, thereby stabilizing the tetragonal phase.

The partially stabilized zirconias (PSZ) are a special topological case of a two-phase composite. They consist of discrete tetragonal precipitates embedded in a cubic matrix so that moisture species have to diffuse through the cubic matrix to reach the tetragonal precipitates and destabilize them. As moisture diffusion through the cubic phase is extremely slow, the kinetics of LTD can be expected to also be slow.[40] This is borne out by the data on PSZ shown in Fig. 5 and underlined in a recent paper on the possible use of Mg–PSZ as a biomaterial.[76]

VII. Open Issues

The major unresolved issue is identifying in details the underlying mechanism by which moisture catalyzes the transformation from *t–m* zirconia. The prevailing explanation in the literature is that moisture, in the form of OH^- ions, diffuses into the zirconia lattice and fills oxygen vacancies,[21,47,77,78] lowering the vacancy concentration and thereby destabilizing the tetragonal phase. The scenario often proposed for the LTD of tetragonal ZrO_2 consists of the following steps[21]:

(i) chemical adsorption of H_2O on ZrO_2 surface,

(ii) reaction of H_2O with O^{2-} on the ZrO_2 surface to form hydroxyl ions OH^-,

(iii) penetration of OH^- into the inner part by grain boundary diffusion,

(iv) filling of oxygen vacancies within the grains by OH^- ions, and therefore formation of proton defects,

(v) occurrence of a *t–m* transformation when the oxygen vacancy concentration is reduced to the extent that the tetragonal phase is no longer stable.

Experimental evidence and atomistic simulations support chemical adsorption and water dissociation.[79] Penetration of "water-derived species" and filling of oxygen vacancies are also clearly established. However, the nature of the diffusing species and of the species filling the oxygen vacancies is still discussed.

According to Yoshimura and colleagues, Guo and Kim (among others), OH^- diffuses and fills oxygen vacancies, and this is supported by XPS, FT-IR observations on polycrystals. The other argument for the role of OH^- ions is that a relatively simple Kroger–Vink equation can be written for the reaction between water and zirconia

$$H_2O + V_0^{\bullet\bullet} + O_O^x \overset{ZrO_2}{\rightleftarrows} 2(OH)_O^{\bullet} \tag{8}$$

where $(OH)_O^{\bullet}$ represents an OH^- ion on an oxygen site in the zirconia lattice.

However, while it is convenient to write such a reaction, it should be noted that it is not the only possible reaction, as discussed below. Moreover, According to the recent work of Doung *et al.*,[80] there is no evidence that OH^- ions are a mobile species in tetragonal zirconia single crystals. SIMS experiments rather point to a separate diffusion of both O^{2-} and H^+ following parallel but independent path into the lattice. Based on much of the literature on solid-state proton conductors, H^+ associates with O^{2-} to form OH^-; but transport of H^+ occurs by hopping between adjacent oxygen ions (Grotthuss mechanism[81]). For this reason, it is to be expected that if there is any oxygen ion transport (which is the case in zirconia), then these

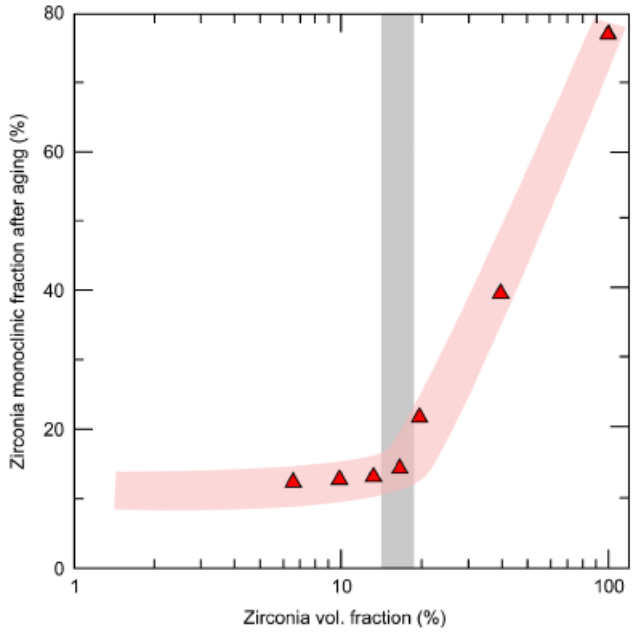

Fig. 10. Monoclinic fraction versus zirconia content in zirconia-toughened alumina composites after 40 h at 140°C in steam. The zirconia phase is a 3Y-TZP. TZP, tetragonal zirconia polycrystals; Y, yttria.

two are independent processes, consistent with SIMS results. That is, in many of the proton conductors, OH^- rarely transport as OH^- ion. An alternative description of the filling of oxygen vacancies by water species is therefore proposed

– dissociation of water into oxygen ions and protons:

$$H_2O \overset{ZrO_2}{\rightleftarrows} 2H^+ + O^{2-}$$

– filling of oxygen vacancies by oxygen ions:

$$2H^+ + O^{2-} + V_O^{\bullet\bullet} \overset{ZrO_2}{\rightleftarrows} 2H^+ + O_O^x$$

where the reaction is buffered by the stabilizer charge compensation reaction

$$Y_2O_3 \overset{ZrO_2}{\rightleftarrows} 2Y'_{Zr} + 3O_O^x + V_O^{\bullet\bullet}$$

If the results presented above may be viewed as contradictory, both may account for zirconia destabilization by a similar process of "filling" oxygen vacancies, and may proceed in series in polycrystalline zirconia (i.e., OH^- diffusion at grain boundaries, then O^{2-} and H^+ diffusion in the lattice).

Also, is should be noted that if diffusion of water species alone were important, then one might expect that the higher the yttria stabilizer content, the larger the diffusional flux would be as there would be a greater number of diffusion paths. However, SIMS data indicate that neither *H* nor *D* ions diffuse in cubic YSZ (that contains high amounts of yttria) at the temperatures associated with LTD.[80] Therefore, further discussion awaits more detailed and critical experimentation.

While it may well be that OH^- (or O^{2-} and H^+) ions play a role in the diffusion mechanism, their role in causing the transformation to monoclinic zirconia has not been made explicit. Filling oxygen vacancies implies that the local coordination of the Zr ions is changed to eightfold coordination but the coordination of Zr ions in monoclinic is sevenfold coordination. So, the transformation also requires that there be a cooperative interaction between many Zr ions. This may be the critical event for the nucleation of the monoclinic phase. Replacing an oxygen vacancy with an OH^- ion satisfies overall local neutrality but also places a proton in the vicinity of a Zr^{4+} ion. The consequences of this on the rearrangement required for the transformation from tetragonal to monoclinic remain to be investigated. Another aspect still requiring clarification is the mechanism or the combination of mechanisms by which the filling of oxygen vacancies results in destabilization of the tetragonal phase. The decrease of oxygen vacancies content, by itself accounts for the destabilization, as discussed before.[22] An alternative process proposed independently by other authors is a stress driven transformation: the filling of oxygen vacancies may be associated to lattice parameters changes, giving rise to stresses in the grains. In this regard, some authors claim that exposure to moisture increases lattice parameters of the tetragonal phase,[46] while others claim that lattice parameters decrease under the same conditions.[47] We would argue that both decrease of oxygen vacancies and accumulation of stresses account for the destabilization. The relative importance of each still remains to be determined.

Diffusion alone is incapable of describing all the features of the TTT behavior, specifically the occurrence of a nose and the kinetics above the nose temperatures. For these reason, we have taken the position in this article that inward diffusion of some moisture-related species provides a necessary but not sufficient condition for the transformation of *t–m* phase. For the transformation to occur there must be a thermodynamic driving force. This is provided by the difference in temperature between the temperature at which the zirconia is exposed to moisture and the T_0 (t/m) temperature. Thus, although the diffusional flux may increase with yttria stabilizer concentration, the T_0 (t/m) temperature decreases and with it the driving force for the transformation.

Although at this time, transformation under electric fields[54] and the effect of reducing atmosphere annealing has been reported to occur, it remains to be studied in sufficient detail to fully explain the observations. Although annealing YSZ in a reducing atmosphere does increase the vacancy concentration the increase is small compared with the total number already in the material to compensate for the stabilizer concentration. It seems more likely that both the reduction treatment and an applied electric field alter the number of free electrons and that, in turn, alters the electrochemical potential for diffusion and hence the kinetics of the transformation. This promises to be a fertile ground for future studies.

Finally, in addition to experimental work on the stability of the tetragonal phase and its transformation, there is a clear need for atomistic simulations of both hydroxyl and hydrogen in zirconia and the role of the effective Fermi level. Knowing and simulating the chemical mechanism of aging would be a powerful tool to create *a priori* new compositions that can exhibit transformation toughening but are insensitive to the presence of water (LTD).

VIII. Summary and Conclusions

Although zirconia has been one of the most important ceramic materials for well over a century, the discovery of transformation toughening heralded new visions for the high-performance applications of zirconia, ranging from biomedical applications to bearing and wear applications. Concurrently and unrelated to transformation toughening but also advanced by new understanding of the role of microstructure, fracture mechanics and phase equilibria of zirconia materials was the development of zirconia SOFC, oxygen sensors, and the implementation of zirconia TBCs. But, in hindsight it is clear that better understanding of the combination of the role of stabilizers, better compositional control, and improved processing all were crucial underpinnings to these new, high technology applications of zirconia. Considering all these factors, YSZ presented the best combination of mechanical properties, low thermal conductivity and high ionic conductivity, and was considered as the premium choice for implants, TBC and SOFC. The current knowledge of LTD, summarized and described in this feature leads us to somewhat revise this superiority of YSZ, because these materials are the most susceptible to isothermal transformation, hence degradation, at low (*in vivo*) or intermediate (up to 400°C) temperatures. They are also prone to phase partitioning at temperatures above 1400°C, which modifies their stability. This combination of aging and phase partitioning has been detrimental for orthopedic applications and may be one limit for the next generation TBCs operating at high temperatures. In this feature, we wanted to highlight the importance of metastable phase diagrams in the design of zirconia-based materials and the impact of LTD on industrial application of YSZ.

Depending on the application, zirconia doped or co-doped with other oxides, or ZTA may present safer alternatives to YSZ. This is the case of biomedical implants, for which the aim is the highest phase transformation under stress (transformation toughening) but the lowest in the presence of moisture (aging). The choice may be more limited for TBC and SOFC, for which low thermal conductivity or high ionic conductivity are directly related to high concentration of oxygen vacancies. The role of oxygen vacancies, and the way they serve as a diffusion path for "water-derived species" remains to be clarified.

References

[1]R. C. Garvie, R. H. J. Hannink, and R. T. Pascoe, "Ceramic Steel," *Nature*, **258**, 703–4 (1975).

[2]A. V. Virkar and R. L. K. Matsumoto, "Ferroelastic Domain Switching as a Toughening Mechanism in Tetragonal Zirconia," *J. Am. Ceram. Soc.*, **69** [10] C224–6 (1986).

[3]D. J. Green, R. H. J. Hannink, and M. V. Swaink, *Transformation Toughening of Ceramics*, pp. 137–44. CRC Press, Bocca Raton, FL, 1989.

[4]O. Ruff and F. Ebert, "Contributions on the Ceramics of Highly Fireproof Material I: The Forms of Zirconium Dioxide," *Z. Anorg. Allg. Chem.*, **180** [1] 19–41 (1929).

[5]M. Yashima, M. Kakihana, and M. Yoshimura, "Metastable-Stable Phase Diagrams in the Zirconia Containing Systems Utilized in Solid Oxide Fuel Cell Applications," *Solid State Ionics*, **86–88**, 1131–49 (1996).

[6]D. R. Clarke and C. G. Levi, "Materials Design for the Next Generation Thermal Barrier Coatings," *Annu. Rev. Mater. Res.*, **33**, 383–417 (2003).

[7]P. Duwez, F. H. Brown, and F. Odell, "The Zirconia–Yttria System," *J. Electrochem. Soc.*, **98** [9] 356–62 (1951).

[8]M. Kilo, M. A. Taylor, C. Argirusis, G. Borchardt, B. Lesage, S. Weber, S. Scherrer, H. Scherrer, M. Schroeder, and M. Martin, "Cation Self-Diffusion of 44Ca, 88Y and 96Zr in Single Crystalline Calcia- and Yttria-Doped Zirconia," *J. Appl. Phys.*, **94** [12] 7547–52 (2003).

[9]H. G. Scott, "Phase Relationships in the Zirconia–Yttria System," *J. Mater. Sci.*, **10**, 1527–35 (1975).

[10]O. Fabrichnaya and F. Aldinger, "Assessment of the Thermodynamic Parameters in the System ZrO_2–Y_2O_3–Al_2O_3," *Zeit. Metall.*, **95** [1] 27–39 (2004).

[11]S. Lakiza, O. Fabrichnaya, M. Zinkevich, and F. Aldinger, "On The Phase Relations in the ZrO_2–$YO_{1.5}$–$AlO_{1.5}$ System," *J. Alloys Comp.*, **420**, 237–45 (2006).

[12]M. Yashima, H. Takashina, M. Kakihana, and M. Yoshimura, "Low Temperature Phase Equilibria by the Flux Method and the Metastable–Stable Phase Diagram in the ZrO_2–CeO_2," *J. Am. Ceram. Soc.*, **77** [7] 1869–74 (1994).

[13]B. K. Kim, S. J. Park, and H. Hamaguchi, "Determination of the Oxygen Self-Diffusion Coefficients in Y_2O_3-Containing Tetragonal Zirconia Polycrystals by Raman Spectrometric Monitoring of the ^{16}O–^{18}O Exchange Reaction," *J. Am. Ceram. Soc.*, **76** [8] 2119–22 (1993).

[14]J. Chevalier, S. Deville, E. Munch, R. Jullian, and F. Lair, "Critical Effect of Cubic Phase on Aging in 3 mol% Yttria-Stabilized Zirconia Ceramics for Hip Replacement Prosthesis," *Biomaterials*, **25**, 5539–45 (2004).

[15]H. M. Ondik, and H. F. McMurdie (eds.), *Phase Diagrams for Zirconium and Zirconia Systems*. American Ceramic Society, Westerville, OH, 1998, ISBN 978-1574980554.

[16]T. K. Gupta, J. H. Bechtold, R. C. Kuznicki, L. H. Cadoff, and B. R. Rossing, "Stabilization of Tetragonal Phase in Polycrystalline Zirconia," *J. Mater. Sci.*, **12**, 2421–6 (1977).

[17]R. C. Garvie, "Stabilization of the Tetragonal Structure in Zirconia Microcrystals," *J. Phys. Chem.*, **82** [2] 218–24 (1978).

[18]M. W. Pitcher, S. V. Ushakov, A. Navrotsky, B. F. Woodfield, G. Li, J. Boerio-Goates, and B. M. Tissue, "Energy Crossovers in Nanocrystalline Zirconia," *J. Am. Ceram. Soc.*, **88** [1] 160–7 (2005).

[19]A. Suresh, M. J. Mayo, W. D. Porter, and C. J. Rawn, "Crystallite and Grain-Size-Dependent Phase Transformations in Yttria-Doped Zirconia," *J. Am. Ceram. Soc.*, **86** [2] 360–2 (2003).

[20]P. Li, I. W. Chen, and J. E. Penner-Hahn, "Effect of Dopants on Zirconia Stabilization—An X-Ray Absorption Study: I, Trivalent Dopants," *J. Am. Ceram. Soc.*, **77** [1] 118–28 (1994).

[21]X. Guo, "Property Degradation of Tetragonal Zirconia Induced by Low-Temperature Defect Reaction with Water Molecules," *Chem. Mater.*, **16** [21] 3988–94 (2004).

[22]S. Fabris, A. T. Paxton, and M. W. Finnis, "A Stabilization Mechanism of Zirconia Based on Oxygen Vacancies Only," *Acta Mater.*, **50** [20] 5171–8 (2002).

[23]P. Li, I. W. Chen, and J. E. Penner-Hahn, "Effect of Dopants on Zirconia Stabilization—an X-Ray Absorption Study: II, Tetravalent Dopants," *J. Am. Ceram. Soc.*, **77** [5] 1281–8 (1994).

[24]K. Kawata, H. Maekawa, T. Nemoto, and T. Yamamura, "Local Structure Analysis of YSZ by Y-89 MAS-NMR," *Solid States Ionics*, **177**, 1687–90 (2006).

[25]F. F. Lange, "Transformation Toughening. 1 Size Effects Associated with the Thermodynamics of Constrained Transformations," *J. Mater. Sci.*, **17**, 225–34 (1982).

[26]Y. Murase and E. Kato, "Role of Water Vapor in Crystallite Growth and Tetragonal–Monoclinic Phase Transformation of ZrO_2," *J. Am. Ceram. Soc.*, **66** [3] 196–200 (1983).

[27]S. Deville, G. Guenin, and J. Chevalier, "Martensite Transformation in Zirconia. Part II. Martensitic Growth," *Acta. Mater.*, **52**, 5709–21 (2004).

[28]J. Eichler, J. Rödel, U. Eisele, and M. Hoffman, "Effect of Grain Size on Mechanical Properties of Submicrometer 3Y-TZP: Fracture Strength and Hydrothermal Degradation," *J. Am. Ceram. Soc.*, **90** [9] 2830–6 (2007).

[29]J. F. Nie and B. C. Muddle, "An Alternative Approach to the Crystallography of Martensitic Transformation in ZrO_2," *Mater. Sci. Eng. A*, **438–440** [Spec. Iss.] 343–5 (2006).

[30]P. M. Kelly and L. R. F. Rose, "The Martensitic Transformation in Ceramics—Its Role in Transformation Toughening," *Prog. Mater. Sci.*, **47**, 463–557 (2002).

[31]S. Deville, G. Guenin, and J. Chevalier, "Martensitic Transformation in Zirconia Part I. Nanometer Scale Prediction and Measurement of Transformation Induced Relief," *Acta Mater.*, **52**, 5697–707 (2004).

[32]S. Deville, H. El Attaoui, and J. Chevalier, "Atomic Force Microscopy of Transformation Toughening in Ceria-Stabilized Zirconia," *J. Eur. Ceram. Soc.*, **25** [13] 3089–96 (2005).

[33]R. M. McMeeking and A. G. Evans, "Mechanics of Transformation-Toughening in Brittle Materials," *J. Am. Ceram. Soc.*, **65** [5] 242–6 (1982).

[34]J. Chevalier, C. Olagnon, and G. Fantozzi, "Subcritical Crack Propagation in 3Y-TZP Ceramics: Static and Cyclic Fatigue," *J. Am. Ceram. Soc.*, **82** [11] 3129–38 (1999).

[35]K. Prettyman, "Ferroelastic Domain Formation and Switching as a Toughening Mechanism in Ceria-Doped Zirconia"; Ph.D. Dissertation, Utah University, Salt Lake City, UT, 1991.

[36]J. Chevalier, B. Cales, and J. M. Drouin, "Low-Temperature Aging of Y-TZP Ceramics," *J. Am. Ceram. Soc.*, **82** [8] 2150–4 (1999).

[37]V. Lughi and D. R. Clarke, "High Temperature Aging of YSZ Coatings and Subsequent Transformation at Low Temperature," *Surf. Coat. Technol.*, **200** [5–6] 1287–91 (2005).

[38]L. Gremillard, J. Chevalier, T. Epicier, S. Deville, and G. Fantozzi, "Modeling the Aging Kinetics of Zirconia Ceramics," *J. Eur. Ceram. Soc.*, **24** [13] 3483–9 (2004).

[39]H. El Attaoui, "Influence du renforcement sur le comportement en fatigue statique et cyclique des céramiques monolithiques de type alumine et zircone (Influence of Toughening on Static and Cyclic Fatigue Behaviour of Monolithic Alumina and Zirconia Ceramics)"; Ph.D. Thesis, INSA-Lyon, France, 2003.

[40]M. M. Nagl, L. Llanes, R. Fernandez, and M. Anglada, "The Fatigue Behaviour of Mg–PSZ and ZTA Ceramics"; pp. 61–76 in *Fracture Mechanics of Ceramics*, Vol. 12, Edited by R. C. Bradt., *et al.* Plenum Press, New York, 1996.

[41]J. Schneider, S. Begand, R. Kriegel, C. Kaps, W. Glien, and T. Oberbach, "Low-Temperature Aging Behavior of Alumina-Toughened Zirconia," *J. Am. Ceram. Soc.*, **91** [11] 3613–8 (2008).

[42]D. Gutknecht, J. Chevalier, V. Garnier, and G. Fantozzi, "Key Role of Processing to Avoid Low Temperature Ageing in Alumina Zirconia Composites for Orthopaedic Application," *J. Eur. Ceram. Soc.*, **27** [2–3] 1547–52 (2007).

[43]H. Tsubakino, K. Sonoda, and R. Nozato, "Martensite Transformation Behavior During Isothermal Aging in Partially Stabilized Zirconia with and without Alumina Additions," *J. Mater. Sci. Lett.*, **12**, 196–8 (1993).

[44]V. Lughi and D. R. Clarke, "Low-Temperature Transformation Kinetics of Electron-Beam Deposited 5 wt.% Yttria-Stabilized Zirconia," *Acta Mater.*, **55** [6] 2049–55 (2007).

[45]S. Deville and J. Chevalier, "Martensitic Relief Observation by Atomic Force Microscopy in Yttria-Stabilized Zirconia," *J. Am. Ceram. Soc.*, **86** [12] 2225–7 (2003).

[46]X. Guo and T. Schober, "Water Incorporation in Tetragonal Zirconia," *J. Am. Ceram. Soc.*, **87** [4] 746–8 (2004).

[47]H. Schubert and F. Frey, "Stability of Y-TZP During Hydrothermal Treatment: Neutron Experiments and Stability Considerations," *J. Eur. Ceram. Soc.*, **25** [9] 1597–602 (2005).

[48]Y. Gaillard, E. Jiménez-Piqué, F. Soldera, F. Mücklich, and M. Anglada, "Quantification of Hydrothermal Degradation in Zirconia by Nanoindentation," *Acta Mater.*, **56** [16] 4206–16 (2008).

[49]J. F. Jue, J. Chen, and A. V. Virkar, "Low Temperature Aging of *t*′-Zirconia: The Role of Microstructure and Phase Stability," *J. Am. Ceram. Soc.*, **74** [8] 1811–20 (1991).

[50]J. Chevalier, L. Gremillard, and S. Deville, "Low-Temperature Degradation of Zirconia and Implications for Biomedical Implants," *Annu. Rev. Mater. Res.*, **37**, 1–32 (2007).

[51]B. Cales, "Zirconia as a Sliding Material: Histologic, Laboratory, and Clinical Data," *Clin. Orthopaed. Relat. Res.*, **379**, 94–112 (2000).

[52]Hip Implants Recalled Because of Potential Fracture Problem, FDA Patient Safety News: Show #2, March 2002, available at http://www.accessdata.fda.gov/scripts/cdrh/cfdocs/psn/printer.cfm?id=107 (accessed on July 28, 2009).

[53]I. Denry and J. R. Kelly, "State of the Art of Zirconia for Dental Applications," *Dent. Mater.*, **24** [3] 299–307 (2008).

[54]S. P. S. Badwal and N. Nardella, "Formation of Monoclinic Zirconia at the Anodic Face of Tetragonal Zirconia Polycrystalline Solid Electrolytes," *Appl. Phys. Sol. Surf.*, **49** [1] 13–24 (1989).

[55]D. J. Kim, H. J. Jung, J. W. Jang, and H. L. Lee, "Fracture Toughness, Ionic Conductivity, and Low-Temperature Phase Stability of Tetragonal Zirconia Codoped with Yttria and Niobium Oxide," *J. Am. Ceram. Soc.*, **81** [9] 2309–14 (1998).

[56]W. C. Jung, J. L. Hertz, and H. L. Tuller, "Enhanced Ionic Conductivity and Phase Meta-Stability of Nano-Sized Thin Film Yttria-Doped Zirconia (YDZ)," *Acta Mater.* **57** [5] 1399–404 (2009).

[57]National Research Council. *Coatings for High Temperature Structural Materials: Trends and Opportunities*. National Research Council, Washington, 1996.

[58]U. Schulz, C. Leyens, K. Fritscher, M. Peters, B. Saruhan-Brings, O. Lavigne, J. M. Dorvaux, M. Poulain, R. Mévrel, and M. Caliez, "Some Recent Trends in Research and Technology of Advanced Thermal Barrier Coatings," *Aerospace Sci. Technol.*, **7**, 73–80 (2003).

[59]W. D. Kingery, H. K. Bowen, and D. R. Uhlmann, *Introduction to ceramics*. Wiley and Sons, New York, 1976.

[60]S. Stecura Optimization of the NiCrAl–Y/ZrO_2–Y_2O_3 Thermal Barrier System. NASA Report TM-86905, 1985

[61]C. Mercer, J. R. Williams, D. R. Clarke, and A. G. Evans, "On a Ferroelastic Mechanism Governing The Toughness of Metastable Tetragonal-Prime Yttria-Stabilized Zirconia," *Proc. R. Soc. Lond. Ser. –Mathematic. Phys. Eng. Sci.*, **463**, 1393–408 (2007).

[62]R. Mevrel, J.-C. Laizet, A. Azzopardi, B. Leclercq, M. Poulain, O. Lavigne, and D. Demange, "Thermal Diffusivity and Conductivity of $Zr1-xY_xO_{2-x/2}$ ($x = 0$, 0084 and 0179). Single Crystals," *J. Eur. Ceram. Soc.*, **24** [10–11] 3081–9 (2004).

[63]S. Deville, J. Chevalier, and L. Gremillard, "Influence of Surface Finish and Residual Stresses on the Ageing Sensitivity of Biomedical Grade Zirconia," *Biomaterials*, **27**, 2186–92 (2006).

[64]P. J. Whalen, F. Reidinger, and R. F. Antrim, "Prevention of Low Temperature Surface Transformation by Surface Recrystallization in Yttria Doped Tetragonal Zirconia," *J. Am. Ceram. Soc.*, **72** [2] 319–21 (1989).

[65]K. Mehta, J. F. Jue, and A. V. Virkar, "Grinding-Induced Texture in Ferroelastic Tetragonal Zirconia," *J. Am. Ceram. Soc.*, **73** [6] 1777–9 (1990).

[66]J. Allain, S. Le Mouel, D. Goutallier, and M. C. Voisin, "Poor Eight-Year Survival of Cemented Zirconia-Polyethylene Total Hip Replacements," *J. Bone Joint Surg. (Br)*, **81-B**, 835–42 (1999).

[67]J. F. Bartolomé, I. Montero, M. Díaz, S. López-Esteban, J. S. Moya, S. Deville, L. Gremillard, J. Chevalier, and G. Fantozzi, "Accelerated Aging in 3-mol%-Yttria-Stabilized Tetragonal Zirconia Ceramics Sintered in Reducing Conditions," *J. Am. Ceram. Soc.*, **87** [12] 2282–5 (2004).
[68]A. V. Virkar, "Transport of H_2, O_2, and H_2O through Single-Phase, Two-Phase, and Multi-Phase Proton, Oxygen Ion and Electron Hole Conductors," *Solid State Ionics*, **140**, 275–83 (2001).
[69]US Food and Drug Administration. "Steam Re-Sterilization Causes Deterioration of Zirconia Ceramic Heads of Total Hip Prostheses, 1997. Available at http://www.fda.gov/MedicalDevices/Safety/AlertsandNotices/PublicHealthNotifications/ucm062472.htm (accessed on July 28, 2009).
[70]T. Sato and M. Shimada, "Transformation of Ceria-Doped Tetragonal Zirconia Polycrystals by Annealing in Water," *Am. Ceram. Soc. Bull.*, **64** [10] 1382–4 (1985).
[71]V. Sergo, C. Schmid, S. Meriani, and A. G. Evans, "Mechanically Induced Zone Darkening of Alumina Ceria-Stabilized Zirconia Composites," *J. Am. Ceram. Soc.*, **77** [11] 2971–6 (1994).
[72]F. M. Pitek and C. G. Levi, "Opportunities for TBCs in the ZrO_2–$YO_{1.5}$–$TaO_{2.5}$ System," *Surf. Coat. Technol.*, **201**, 6044–50 (2007).
[73]Q. Ma, W. Pompe, J. D. French, and D. R. Clarke, "Residual-Stresses in Al_2O_3–ZrO_2 Composites—a Test of Stochastic Stress Models," *Acta Met. Mater.*, **42** [5] 1673–81 (1994).
[74]C. Pecharromán, J. F. Bartolomé, J. Requeña, J. S. Moya, S. Deville, J. Chevalier, G. Fantozzi, and R. Torrecillas, "Percolative Mechanism of Aging in Zirconia-Containing Ceramics for Medical Applications," *Adv. Mater.*, **15** [6] 507–11 (2003).
[75]R. Zallen, *The Physics of Amorphous Solids*. Wiley, New York, NY, 1983 ISBN: 978-0-471-29941-7.
[76]M. E. Roy, L. A. Whiteside, B. J. Katerberg, J. A. Steiger, and T. Nayfeh, "Not all Zirconia Femoral Heads Degrade In Vivo," *Clin. Orthop. Rel. Res.*, **465**, 220–6 (2007).
[77]T. T. Lepisto and T. A. Mäntylä, "A Model for the Structural Degradation of Y-TZP Ceramics in Humid Atmosphere," *Ceram. Eng. Sci. Proc.*, **10**, 658–67 (1989).
[78]M. Yoshimura, T. Noma, K. Kawabata, and S. Somiya, "Role of H2O on the Degradation Process of Y-TZP," *J. Mater. Sci. Lett.*, **6** [4] 465–7 (1987).
[79]S. E. Redfern, R. W. Grimes, and R. D. Rawlings, "The Hydroxylation of *t*-ZrO_2 Surfaces," *Journal of Materials Chemistry*, **11** [2] 449–55 (2001).
[80]T. Doung, A. Limarga, and D.R Clarke, *J. Am. Ceram. Soc.* in press.
[81]N. Agmon, "The Grotthuss Mechanism," *Chem. Phys. Lett.*, **244**, 456–62 (1995).

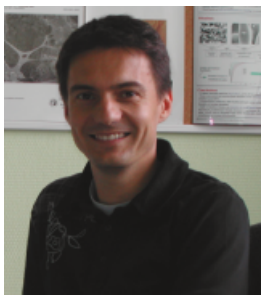

Born in 1970, Jérôme Chevalier is currently full Professor at the National Institute of Applied Sciences (University of Lyon), in France. After receiving his Ph.D. in 1996 (mechanical properties of biomedical grade zirconia), Jérôme Chevalier first became Ceramic Engineer in Saint Gobain Group, responsible for the R&D activity on biomedical applications of ceramics. In 1997, he joined the National Institute of Applied Sciences, in Villeurbanne, as assistant professor, then full professor in 2004. He is in charge of the ceramic group of the materials department (14 permanent researchers, 20 Ph.D.). His research activity is now mainly focused on bioceramics, from their processing to their mechanical and biological properties. His research interests include new generations of zirconia-based composites in orthopedics and dentistry, nanostructured ceramics and composites, hybrid organic–inorganic composites and bioactive glasses and ceramics for tissue engineering. He has published more than 80 international papers with a review process, and six review papers in journals and encyclopedia.

Laurent Gremillard is a Research Scientist at the National Centre for Scientific Research (CNRS). He received his engineering degree and his Ph.D. from the National Institute of Applied Science (INSA) in Lyon (France) in 1998 and 2002, respectively. He then was post doctoral fellow at the Lawrence Berkeley National Laboratory for 2 years, where his research was focused on the behaviour of lead-free solders on ceramic surfaces. He joined CNRS in October 2004, and is currently working in the ceramic group of the Materials, Engineering and Science laboratory (joint laboratory between INSA-Lyon and CNRS). He is interested in every aspect of bioceramics, from processing to mechanical, microstructural and biological characterization. He currently works on zirconia ceramics and composites, and on organic–inorganic porous composites for bone substitution. He has authored or coauthored around 25 scientific papers in peer-reviewed materials science journals.

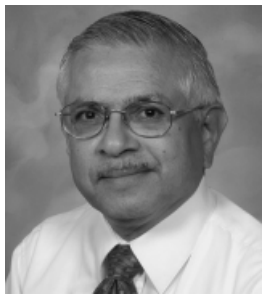

Anil Virkar is Distinguished Professor and Chair of the Department of Materials Science & Engineering at the University of Utah. He received B.Tech. (Hons.) in Metallurgical Engineering from Indian Institute of Technology, Mumbai, India (1967); M.S. in Engineering Mechanics from Louisiana State University in (1969); and Ph.D. in Materials Science from Northwestern University in (1973). He is a Fellow of the American Ceramic Society, a Fellow of The Electrochemical Society, and a member of the American Society for Metals, American Chemical Society, and Materials Research Society. His research interests are in ceramics, ionic and electronic conductors, fuel cells, batteries, solid-state electrochemistry, renewable energy, sensors, transport, thermodynamics of high-temperature materials, and fracture of materials. He has published over 250 papers and is an inventor or coinventor on over 40 patents.

David R. Clarke is Gordon McKay Professor of Materials and Applied Physics in the Harvard School of Engineering and Applied Sciences, Harvard University, Cambridge, USA. He is also an Honorary Visiting Professor at Imperial College, London.

He holds a Ph.D. in Physics from the University of Cambridge, a B.Sc. degree in Applied Sciences from Sussex University, UK and was awarded a Sc.D. from the University of Cambridge. Before moving to Harvard, he was professor of materials at the University of California, Santa Barbara (1990–2008). Previous positions include being senior manager, IBM Research Division, Yorktown Heights (1983–1990), associate professor, Massachusetts Institute of Technology (1983), group leader, Rockwell International Science Center (1977–1983) and senior scientific officer, The National Physical Laboratory, Teddington, UK. He has published over 450 papers and holds five patents. David Clarke is a member of the National Academy of Engineering, a Fellow of the American Physical Society, and received an Alexander von Humboldt Foundation Senior Scientist Award.

A member of the Basic Science Division since joining the society in 1976, David Clarke has been chair of the Basic Science Division as well as a trustee of the society, and an associate editor of the *Journal of the American Ceramic Society*. He has received the Sosman Award, the Richard M. Fulrath Memorial Award, Edward Henry Award, and Ross Coffin Purdy Award, and was elected a Fellow of the Society in 1985. He was recently listed as author of one of the 11 best papers in the 110 years of publication of the Journal. □